Wax based Bio-MEMS Device for Drug Delivery

by
Parth Ujjaval Patel

A thesis submitted to Johns Hopkins University in conformity with the requirements for the degree of Master of Science in Engineering

Baltimore, Maryland
December, 2015

Abstract

The term “sustained drug release” first appeared in 1953 when scientists attempted to use alkaloids and ion exchange to retard the release of drugs from capsules. The main motivation behind sustained drug release was to ensure that the drug was in contact with the stomach and intestine lining for as long as possible. Today, the motivation for using sustained drug release tablets has shifted to helping clinicians increase patient compliance. A 2002 study found that sustained-release of Glipizide, an oral drug for Type 2 diabetes, increased adherence indices by 60%. Current drug release systems, however, have not evolved and are limited by the tablet degradation properties. Engineers have not been able to consistently develop oral drug delivery devices that can last for more than 72 hours.

We propose to develop a 500 micron sized metallic theragripper composed of a chromium/copper stress bilayer, a gold rigid layer and a paraffin wax trigger layer. The paraffin wax trigger layer can serve as a sustained controlled drug delivery component. This study aims to begin examining the development of a system that uses paraffin wax as a drug delivery component. In order to do so, we examined some previous wax drug delivery systems along with our own experiments. Successful completion of this initial study will provide future engineers with direction when attempting to develop safe, scalable and effective drug delivery devices based on paraffin wax.

Advisor: Dr. David Gracias Reader: Dr. Honggang Cui

Acknowledgements

I would like to thank everyone who has helped me throughout my time at Hopkins, both during my undergraduate and graduate education. First, I would like to thank my parents for supporting me in every single way possible to make it easier for me to focus on my education and obtaining my degree. My professors over the past four to five years have been some of most amazing and intelligent people I have had the pleasure of interacting with. In particular, I am grateful for the guidance and direction that Dr. Gracias and Dr. Cui provided me throughout my education. In addition, I would like to thank Dr. Sravanti Kusuma, a former Ph.D candidate for her mentorship during my undergraduate research experiences. Lastly, I would like to thank Dr. Arijit Ghosh, a postdoctoral student who provided me with advice and guidance for my Master's project.

Table of Contents

Chapter 1: Introduction to Controlled Drug Delivery

Controlled drug delivery has been the motivation for various research fields and has grown even more rapidly with the introduction of micro/nanoscale drug delivery devices. Localized and systemic controlled drug delivery devices are of great interest to the medical and biomedical community. Mark Saltzman defines controlled drug delivery as "(1) includ[ing] a component that can be engineered to regulate an essential characteristic and (2) have a duration of action longer than a day."[1] Controlled drug delivery allows for both spatial and temporal delivery of drugs, whereas sustained release allows for a more prolonged release of drugs.

1.1 Background

Controlled release devices provides clinicians with an alternative to increase patient compliance.[2] Diabetes mellitus type 2 affects 366 million people worldwide.[3] For those patients on oral hypoglycemic drugs, the average adherence rate is around 40%-

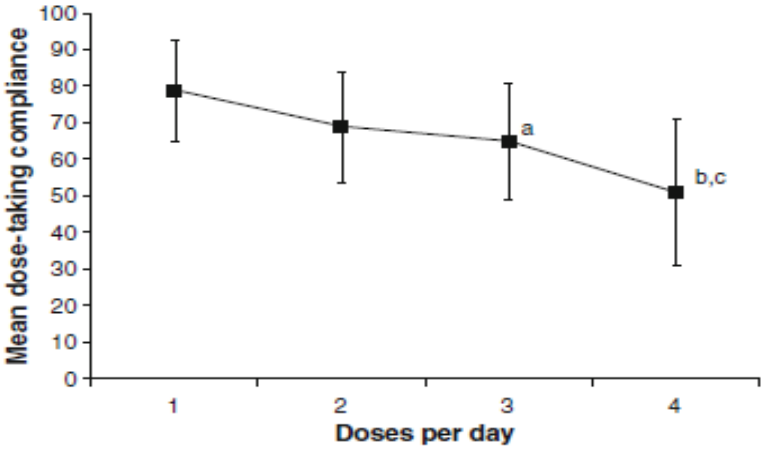

Figure 1: Reduced Adherence with Increased Dose Frequency. Claxton et al. performed an extensive review of published reports to find that as dosing frequencies increase, adherence rates decrease.[7] "[a]Once daily vs. three-times daily, $P = 0.008$. [b]Once daily vs. four-times daily, $P < .001$. [c]Twice daily vs. four-times daily, $P < 0.001$."[6] Reprinted with permission from Springer. Copyright 2013.

46%.[4,5] Recent studies have shown that a large factor for reduced adherence in patients taking oral hypoglycemic drugs is increased dosing frequency.[6,7]

In addition to the potential for increased patient compliance, controlled drug release reduces 'see-saw' concentration fluctuation. With traditional immediate release drug delivery systems, there is a fluctuation in drug concentration in systematic circulation as well as in body compartments. These fluctuations are dependent on basic drug kinetics.[2] 'See-saw' fluctuations can affect a drugs ability to stay within the minimum toxic concentration (MTC) and minimum effective concentration (MEC) window.[8] In order to minimize side effects, drug concentration must remain below MTC, however in order for the drug to maintain therapeutic benefit, drug concentration must remain above the MEC.[9]

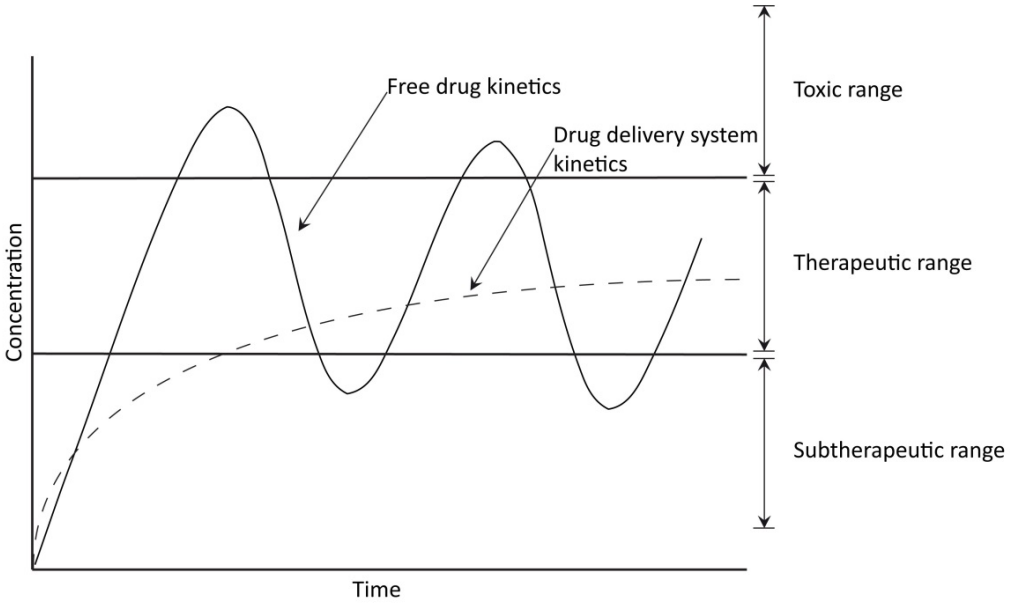

Figure 2: Immediate vs. Controlled release. Controlled release devices allow for optimization in order to maintain drug concentration within the therapeutic range. Overall, this allows for reduction in side effects.[9]

Controlled drug delivery also reduces the overall necessary dose. This leads to fewer systematic and local side effects. Furthermore, reduced dosage is of great economic benefit as the price per unit for the drug is greatly reduced. This, in turn, can lead to an increase in patient compliance. Zeng et al., found that a 33% reduction in cost for diabetic medications led to a 7.3% increase in adherence.[10]

Yet another advantage controlled drug delivery offers is improved treatment efficiency. With systematic immediate release doses, the drug action pervades all organs and tissue in the body. This can lead to undesirable side effects and an increase in risk to patients with existing alternate conditions. A controlled release drug delivery device can manage the overall drug concentration for acute and chronic conditions.[2]

A particular challenge of controlled drug delivery is a phenomenon called dose dumping. Dose dumping would result from a malfunction in the drug delivery device where the stored dosage would be rapidly released into systematic circulation. This could potentially lead to fatalities, especially in potent drugs with a small MEC-MTC window.[2]

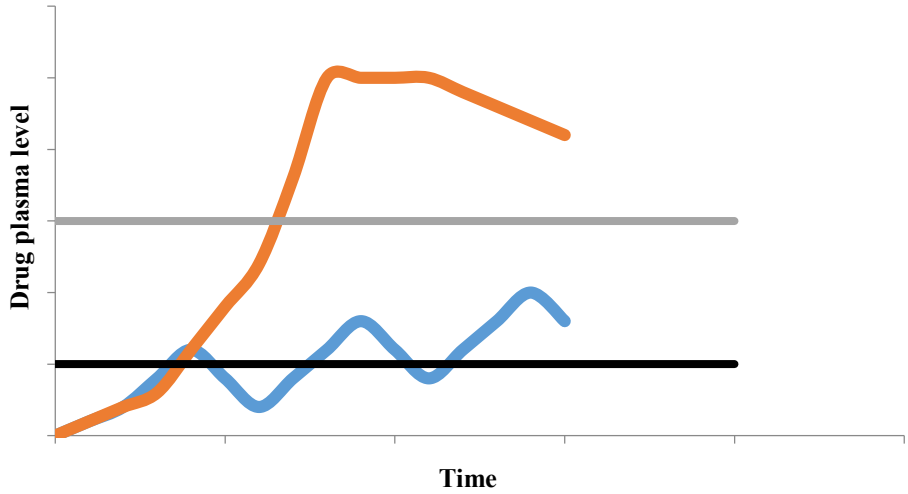

Figure 3: Immediate Dose Release vs. Dose Dumping Device. A malfunctioning controlled drug delivery device that is dose dumping (orange) will surpass the minimum toxic concentration (gray) and maintain a drug plasma level at a dangerously high concentration. Immediate drug release systems (blue) carry a short life-span and dose so they can remain above the minimum effective concentration (black) yet stay below the MTC.

Another challenge of controlled drug delivery is a limited dosing flexibility for the prescriber and patient. Current oral drugs allow for the patient or provider to alter the drug dose by fracturing tablets or capsules into multiple pieces. This greater flexibility provides for simpler dose adjustments. With controlled drug delivery devices, there will need to be a greater variety of doses available to each patient. This leads to reduced flexibility. For example, some patient suffering from diabetes may not need a full dose on any given day. The dose required for these patients could fluctuate daily. Controlled drug delivery devices will not provide similar flexibility. Fracturing controlled drug delivery devices could make them more susceptible to dose dumping as the controlled release material property could be compromised if fractured.[2]

Many controlled drug delivery systems follow diffusion kinetics. The drugs are encapsulated in high concentrations in either a reservoir or matrix system. The drug particles then move from a region of high concentration to the boundary layer, where there is a low concentration. The flux (J) of the drug across the given boundary of the delivery system is characterized by Fick's law.[2]

$$J = -D\frac{dc}{dx} \qquad \text{[Equation 1]}$$

Where D is the diffusion coefficient and dc/dx is the change in concentration (c) over distance (x). Furthermore, when the drug is encapsulated in a water insoluble membrane, it must travel through membrane and thus the drug release rate (dm/dt) is defined by Equation 2.[2]

$$\frac{dm}{dt} = \frac{ADK\Delta C}{L} \qquad \text{[Equation 2]}$$

Here, A and L are the area and thickness of the membrane layer, respectively. K is the partition coefficient of the drug between the boundary membrane layer and the high concentration drug core while ΔC is the concentration difference over the membrane.[2]

1.2 Reservoir Type System

Reservoir delivery systems are becoming an increasingly popular choice for sustained drug delivery. The drug release rate is controlled by the polymer properties and the thickness of the coating. In addition, the physicochemical properties of the drug, such as solubility, drug particle size and molecular weight, play a large role on the drug release kinetics from the polymer layer.[11,12] Reservoir systems are most useful for sustained drug

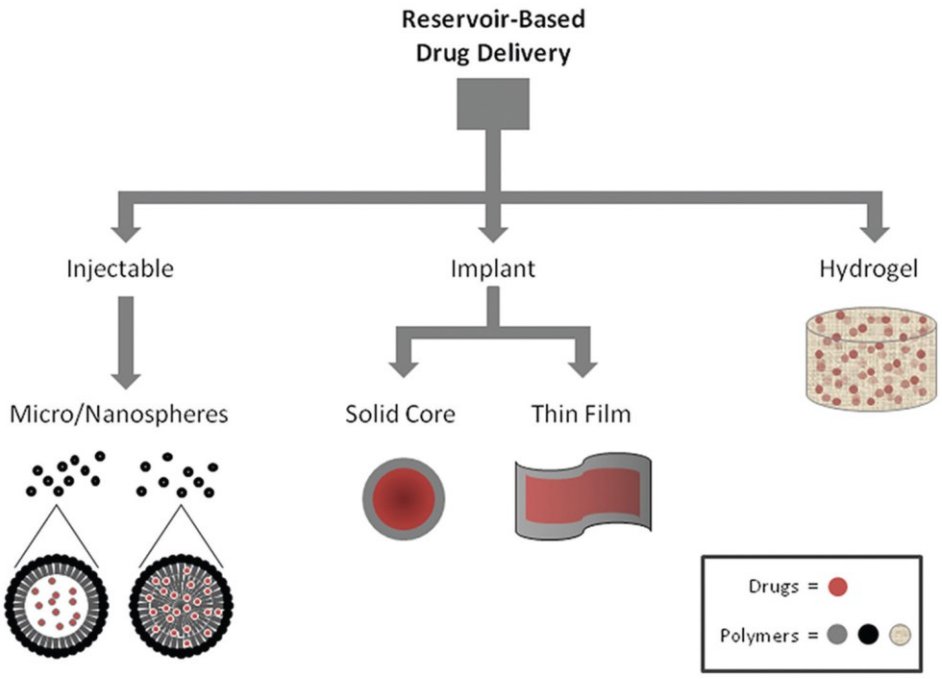

Figure 4: Reservoir system categories. Various systems can be used for reservoir drug delivery. Hydrogels provide a multitude of possibilities. Implants are now being researched as long-term systemic drug delivery systems. Injectable options, such as micro/nanospheres are considered versatile drug delivery systems, offering both systemic and targeted drug therapy.[13] Reprinted with gratis reuse permission from Sage Publications. Copyright 2012.

delivery to a localized region or long-term systematic administration.[13] Systematic administration is usually accomplished using a subcutaneous or intramuscular injection or implantation. Based on the shape and structure of the reservoir system, they can be classified into the categories depicted in Figure 4.

Implantable systemic stand-alone reservoir-based drug delivery systems offer a unique option for controlled drug delivery. Often, the implant is surgically placed which can be invasive and carry associated risks such as inflammation or infection. There are some implants that can be taken orally to provide long-term systemic controlled drug delivery through the gastrointestinal tract. The polymers used in these systems must be "biostable, nonbiodegradable, biocompatible and stable in contact with metals."[13] For example, in the 1980s, the Medtronic Corporation's pacemakers were insulated using polyurethane. Over time the polyurethane degraded, leading to inflammatory and fibrotic reaction. In 2002 Boston Scientific Corporation introduced poly(styrene-*block*-isobutylen-*block*-styrene; SIBS).[13] SIBS is a biostable thermoplastic polymer that has the properties of both silicone and polyurethane.[14]

1.3 Matrix Type System

Matrix type systems involve using an insoluble polymer matrix, such as a hydrogel, to optimize the rate of drug diffusion from the delivery system. The mass of drugs released per unit area at time *t* is characterized by the Higuchi equation.[15]

$$Q = \sqrt{\frac{D\emptyset}{T}(2A - \emptyset C_s)t} \qquad \text{[Equation 3]}$$

Where:

Ø represents the porosity of the matrix

C_s is the solubility of the drug in the release medium

T is the tortuosity of the matrix

A is the concentration of drug in the matrix

D is the diffusion coefficient of the drug in the medium surrounding the matrix

Monolithic matrix systems require the drug to be encapsulated or blended into the matrix. These systems can depend on hydrophobicity, hydrophilicity, and solubility to control the rate of drug delivery.[16]

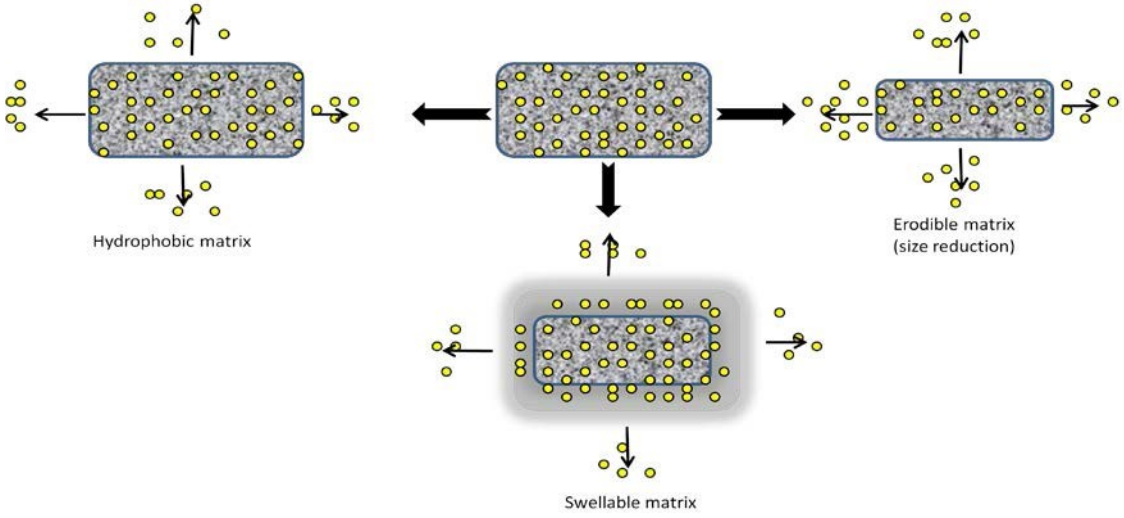

Figure 5: Drug release from varying matrix types. Hydrophobicity can play a role in driving drug release. Erodible matrices behave similarly to dissolvable tablets. Swellable matrices may offer unique smart polymer action.[16]

For systems with partially soluble membranes encapsulating the drug particles, the release rate is characterized by Equation 4.[2]

$$Release\ rate = \frac{AD}{L} = [C_1 - C_2] \qquad \text{[Equation 4]}$$

Where:

A is the Area of the membrane

D is the diffusion coefficient

C_1 is the drug concentration in the matrix

C_2 is the drug concentration in the surrounding medium

L is the diffusional path length

The release rate relies mainly on diffusion and thus with these matrix type systems, the drugs are placed in the matrix following two approaches. The first approach is encapsulating the drug in an insoluble matrix. This allows for the surrounding medium to penetrate the matrix and allow the drug to diffuse out of the matrix. The surrounding medium or solvent drives the diffusion of drugs. The second approach is encapsulating the drug in a polymer coat. In this case, the outer polymer coat is dissolved by the surrounding medium allow the drug to diffuse out through the now liquid boundary layer into the surrounding fluid.[2]

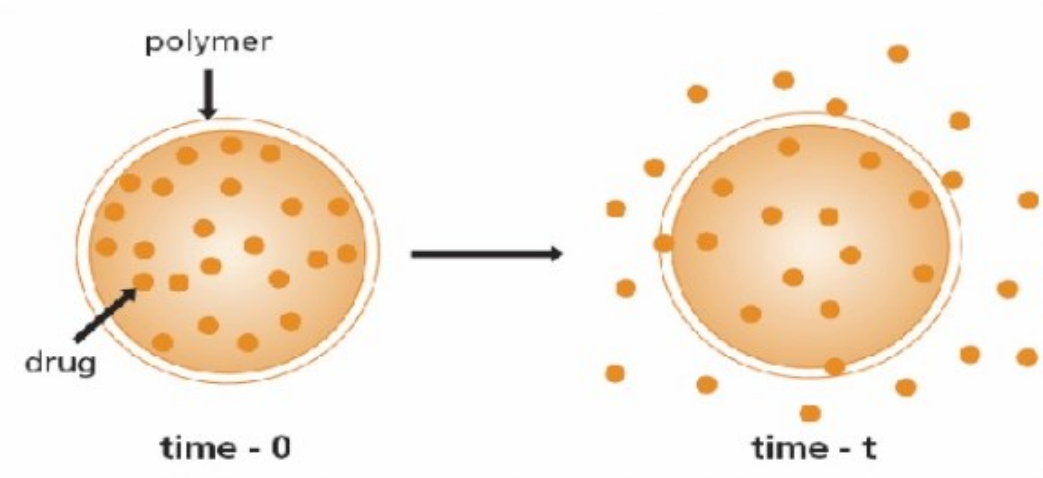

Figure 6: Polymer coat approach for matrix drug delivery. The polymer coat will dissolve over time t and leave behind a liquid boundary layer through which the drug will diffuse.[2]

1.4 Hydrogel type system

Hydrogels offer unique properties due to their hydrophilic insoluble nature. They are capable of absorbing large quantities of water in their network layers. Since they are porous, water-absorbing materials, drug diffusion rate is dependent on the extent of cross-

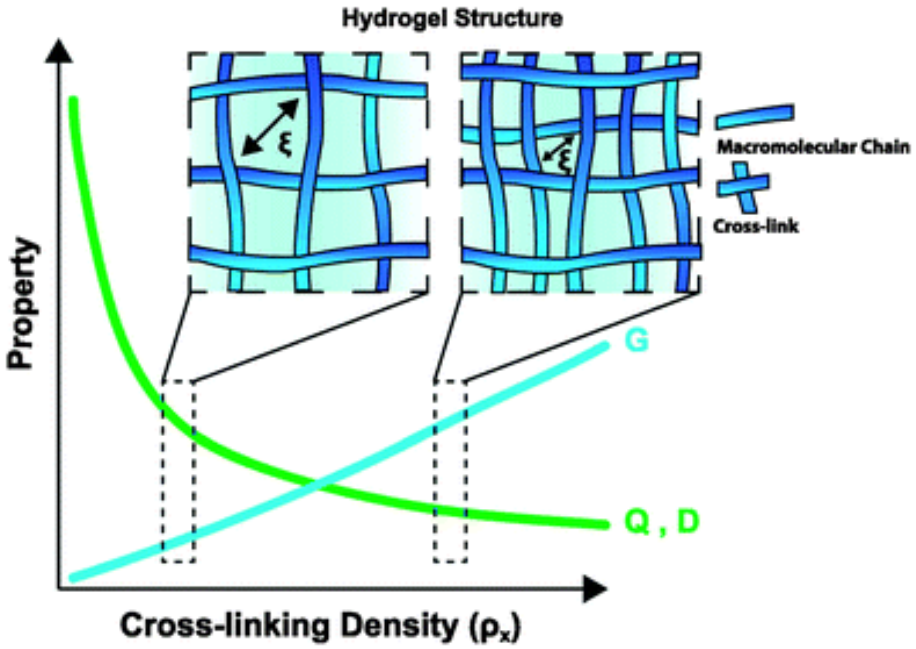

Figure 7: Hydrogel cross-linking density effect on physical properties. As cross-linking density increases, so does the modulus (G). The equilibrium swelling ratio (Q), drug diffusivity (D) and mesh size (ξ) decrease, however, with increasing cross-linking density.[19] Reproduced from Ref 19 with permission from The Royal Society of Chemistry. Copyright 2013.

linking. Cross-linked polymers give the hydrogel a large variety of networks chains for the drug particles to flow through.[1] Cross-linking primarily prevents molecules from dissolving into the surrounding water. Instead, cross-linked polymers will cause the hydrogel to swell as the material enters the network. Hydrogel swelling is limited by the extent of cross-linking and thus the more cross-linked a hydrogel, the more it will swell.[17–19]

Chapter 2: Factors to Consider

Factors that affect drug release rate include: "drug characteristics, polymer variables factors, and the formulation aspects."[20]

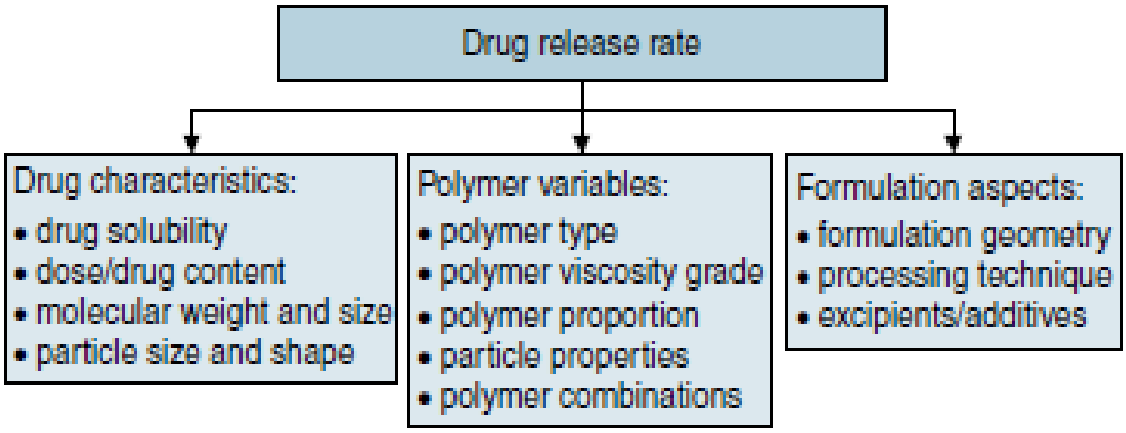

Figure 8: Factors to consider for controlled drug delivery. These three factors can affect the release rate and controllability of a drug delivery system.[20] Reprinted with permission from Springer. Copyright 2004.

2.1 Drug-Related Factors

Drug solubility plays an important role in how readily the drug will diffuse out of a given matrix. These problems can be fixed by adjusting the matrix with surfactants.[20,21] Drug solubility can also affect the mechanism of matrix erosion due to particle displacement. Decreased drug solubility leads to increase erosion of the matrix since the matrix network could segment from the dispersion of insoluble drug particles.[20] In particular, solid particles will reduce swelling of a matrix by entangling the polymer network. Generally, soluble drugs will promote swelling while poorly soluble drugs will prevent swelling and thus lead to erosion.[20,22]

In addition to drug solubility, dosing and drug loading can also affect the drug release kinetics. Increased drug content will increase the rate of release since there is a larger concentration and thus a greater gradient. Equation 5 characterizes the volume fraction of a drug (γ_{ds} in cm^3_{drug}/cm^3_{gel}) at the gel layer.[20,23]

$$\gamma_{ds} = \frac{C_s \gamma_w}{\varepsilon_d} \qquad \text{[Equation 5]}$$

Where:

C_s is drug solubility in water

γ_w is the water volume fraction at the gel layer

ε_d is the drug density

Again, when the drug solubility is low, the polymer erosion will play a larger role in drug release kinetics. In general, the release rate is proportional to the drug solubility-drug loading ratio.[20,24]

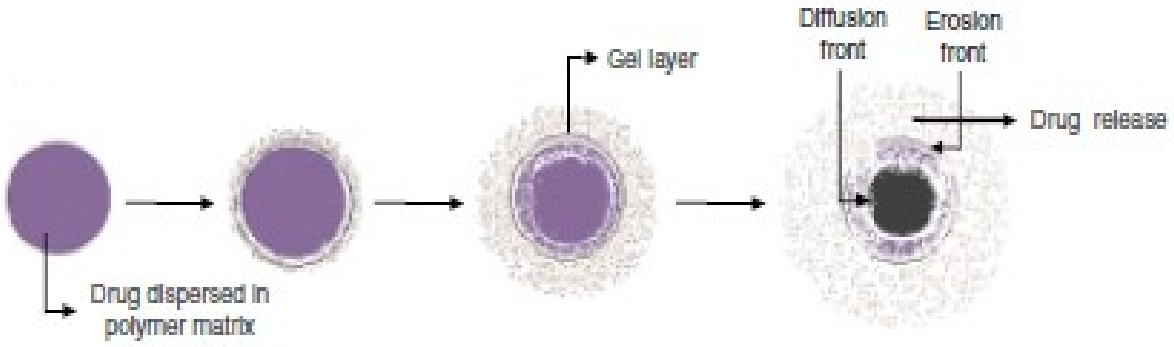

Figure 9: Drug release from a swellable matrix. As the matrix hydrates in the presence of water, both a gel layer and erosion front start to develop around the drug reservoir. These two properties of matrices play a large role in diffusion kinetics.[20] Reprinted with permission from Springer. Copyright 2004.

A drug's molecular weight, particle size and particle shape can play a significant role in the kinetics of the delivery system. The erosion zone and gel layer kinetics is

governed by the diffusion coefficient of a drug. Diffusion coefficients can vary among different matrices to being nearly zero in a dry matrix and reaching a maximum in a hydrated matrix.[20] The Higuchi equation (see Equation 3) dictates that the drug release rate from a matrix based model is proportional to the square root of the diffusion coefficient. The diffusion coefficient depends on molecular weight, particle diameter and matrix viscosity. Furthermore, in general, drugs with molecular weights of >500Da are suspected to be poorly diffusible out of hydrophilic matrices due to the constraining nature of aqueous gel structures.[20,25]

2.2 Polymer-Related Factors

Polymer properties arguably play the largest role in drug release kinetics for controlled release drug delivery systems. Drug release depends on both its ability to diffuse through the matrix as well as the rate of polymer erosion. As the free volume of the polymer increases, so does drug diffusivity. Drug diffusivity is also dependent on the thermodynamic relation between the specific drug particles and the polymer matrix. Polymer variability can be dependent on its "chemical nature, type and degree of substitution, cross-linking, and molecular weight."[20]

Development of a controlled release drug delivery system begins with selecting the best polymer type for the desired drug release kinetics and mechanism. In the past, silicon derivatives were used for fabrication of controlled-release systems, however, more recently, there has been a shift to using water-soluble and biodegradable polymers. Polymers can be defined as "high molecular weight molecules made up of monomer units

with unique properties attributed to their size and three-dimensional arrangement."[20] Generically, there are two broad categories for polymers: water-soluble and water-insoluble.

In hydrophobic matrices, drug is released through aqueous pores in the matrix network. In hydrophilic matrices, drugs migrate through a gel layer before being deposited into the target site. These differences between water-soluble and water-

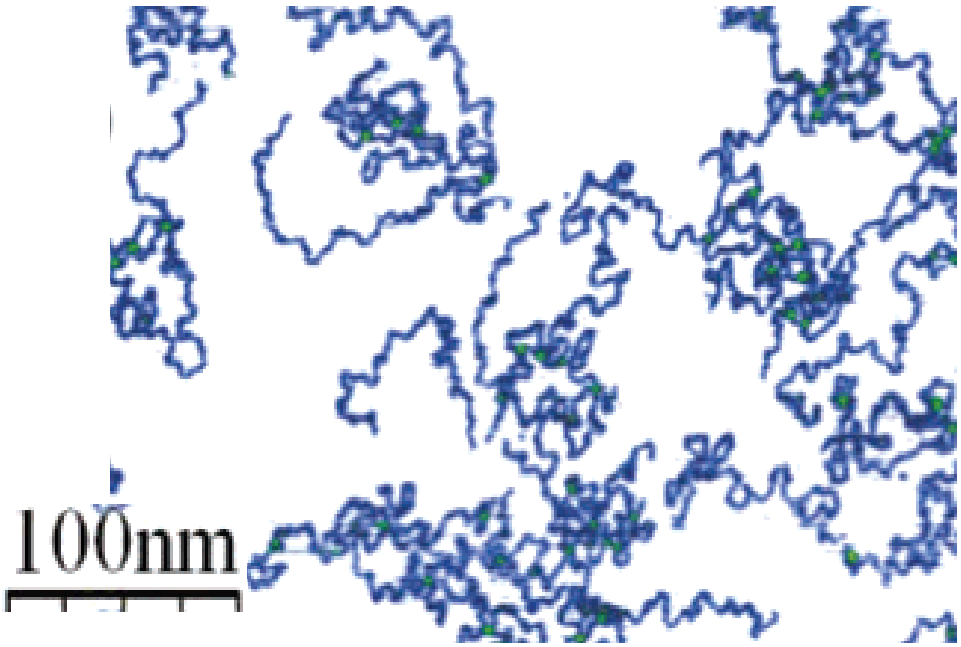

Figure 10: Atomic Force Microscopy image of poly(2-vinylpyridine) (P2VP) polymer chains.[172] Reprinted with permission from the American Chemical Society. Copyright 2005.

insoluble polymers can play a large role in determining release kinetics for drugs. In addition, the polymer's ionic and chemical composition can interact with drug particles to drastically influence the release kinetics.[20,26] Furthermore, physicochemical properties can affect the formation and stability of a gel layer in hydrophilic matrices like Carbopol. Studies have shown that the gel layer propagates much quicker when loaded with basic drugs compared to acidic drugs indicating a pH-dependence on the gelation of

Carbopol.[20,27] Alternatively, some polymers, such as Chitosan, tend to interact with anionic drugs.[28] Other polymers may indicate stereo-selective interactions of functional groups of the drug and polymer which can alter release rates as well.[20,29,30]

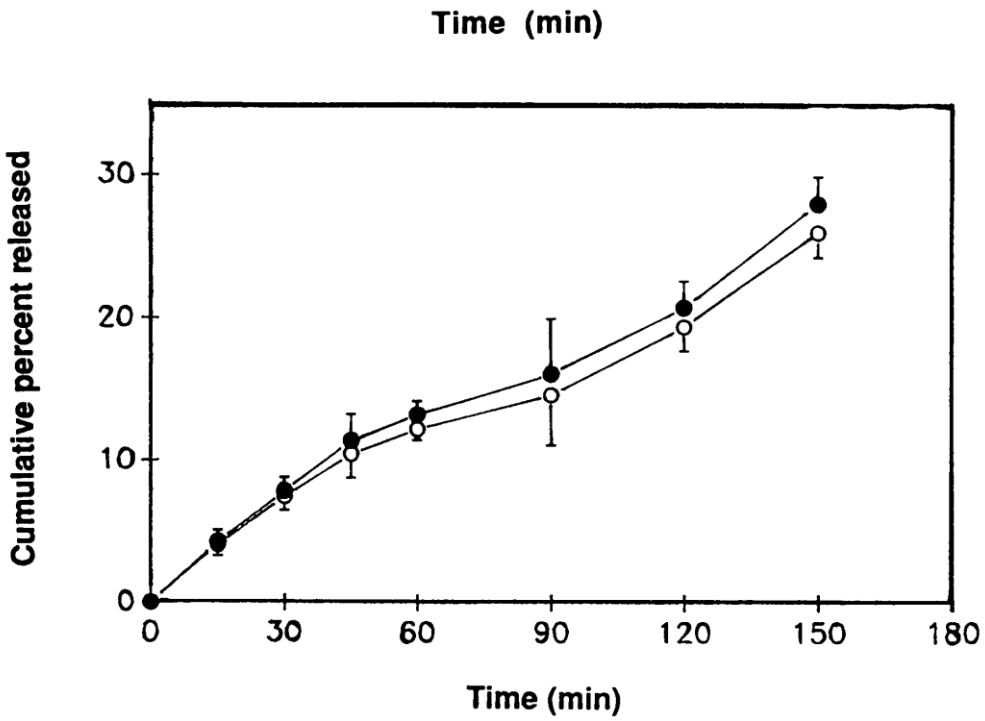

Figure 11: Cumulative kinetic release of (R)-propranolol hydrochloride (open circles) versus (S)-pronanolol hydrochloride (filled circles). HPMC matrices exhibit a slight preference for dissolution of (S)-propranolol hydrochloride as opposed to (R)-propranolol hydrochloride.[30] Reprinted with permission of Springer. Copyright 1993.

Other important physicochemical properties include: polymer viscosity, gel point, hydration rate and glass transition temperature. Figure 12 lists these properties for a variety of widely used polymers in controlled release drug delivery systems.

Polymer	Types/grades	Molecular weight (Da)	Glass transition temperature (°C)	Viscosity (mPa × s)	Solubility
Hydroxypropyl-methylcellulose	Methocel™ K Methocel™ E Methocel™ A	10 000–150 0000	170–180	2–120 000 for 2% w/v aqueous solution at 20°C	Soluble in cold water, in mixture of methanol and ethanol, and in dichloromethane
Hydroxyethyl-cellulose	Natrosol® HHR, H4R, h, MHR, JR, LR	ND	135–140	2–20 000 for 2% w/v aqueous solutions	Soluble in hot and cold water
Hydroxypropyl-cellulose	Klucel® GF, JF, LF, EF, HF	80 000–1 150 000	130	1500–3000 for 1% w/v aqueous solution in Klucel HF	Soluble in methanol, ethanol, and dichloromethane
Carbomer	Carbopol® 934 Carbopol® 934P Carbopol® 971P Carbopol® 1342	1–4 × 10^6	100–105	10 000–100 000 for 1% w/v in 7.4pH buffer	Soluble in water and ethanol after neutralization
Xanthan gum	Xantural® 75	2 × 10^6	82–85	1200–1600 for 1% w/v solution at 25°C	Soluble in old and warm water
Ethylcellulose	Ethocel™ Std 4 to 100 Premium	ND	129–133	4–110 for 5% w/v solution	Insoluble in water, glycerol, and glycols
Carageenan	k-Carageenan λ-Carageenan	ND	ND	5 at 75°C	Soluble in water at 80°C
Polymethacrylates	Eudragit® RS, RL, NE	≥100 000	ND	≤15	Insoluble in water; soluble in alcohols and acetone
Poly-(ethylene oxides)	Polyox™ WSR -N60K -303NF	100 000–7 000 000	60	30–10 000 (depending upon grades) at 25°C	Soluble in water, acetonitrile, chloroform, methylchloride

Figure 12: Physicochemical properties of widely used polymers in controlled drug delivery systems. This figure is a compilation of important physicochemical properties for commonly used polymers.[20] Reprinted with permission from Springer. Copyright 2004.

mPa: Millipascal; ND: no data; s: seconds; w/v: weight/volume

In addition to selecting the correct type of polymer, it is important to keep in mind the polymer viscosity grade. Polymers can be synthesized at various viscosities and often times the viscosity grade is selected during the controlled release delivery system fabrication process. The viscosity of the polymer will dictate the release rate from the matrix by altering the diffusivity and mechanical properties of the gel or erosion layers.[20,31] At higher viscosity grades, matrices are faster hydrating and thus develop a mechanically strong gel layer relatively quickly. This can limit the amount of drug initially released, minimizing the burst effect, while also allowing for an overall longer period of drug release.[20,32] Mechanically stable gel layers tend to be more tortuous and thicker thus decreasing the drug's diffusion coefficient.[20,33] In addition to the viscosity of the polymer, matrices that are substituted with hydration enhancing materials can develop a multitude of gel layers. This is due to increased or decreased water uptake based on the degree of substitution which can decide the final gel structure.[20,31,34,35] Rheology plays a role in the degradation and deformation of matrices. Studies have found a linear relationship between polymer viscosity for the 50% release of verapamil hydrochloride. This relationship was also reported between the furosemide release rate a varying viscosity and concentration of hydroxypropyl methylcellulose (HPMC).[20,36] Lastly, the drug itself can affect the viscosity of the polymer. For example, the drug Nicotinamide forms hydrogen bonds with hydrophilic groups of HPMC thus having a "salting-in" effect on the polymer. This expands the polymer chains, increasing the viscosity, gelation temperature and cloud point. This type of interaction between a drug and polymer can result in a decrease in molecular mobility. Additionally, this interaction can alter the glass transition temperature which can have a drastic effect on the release rate.[20,37]

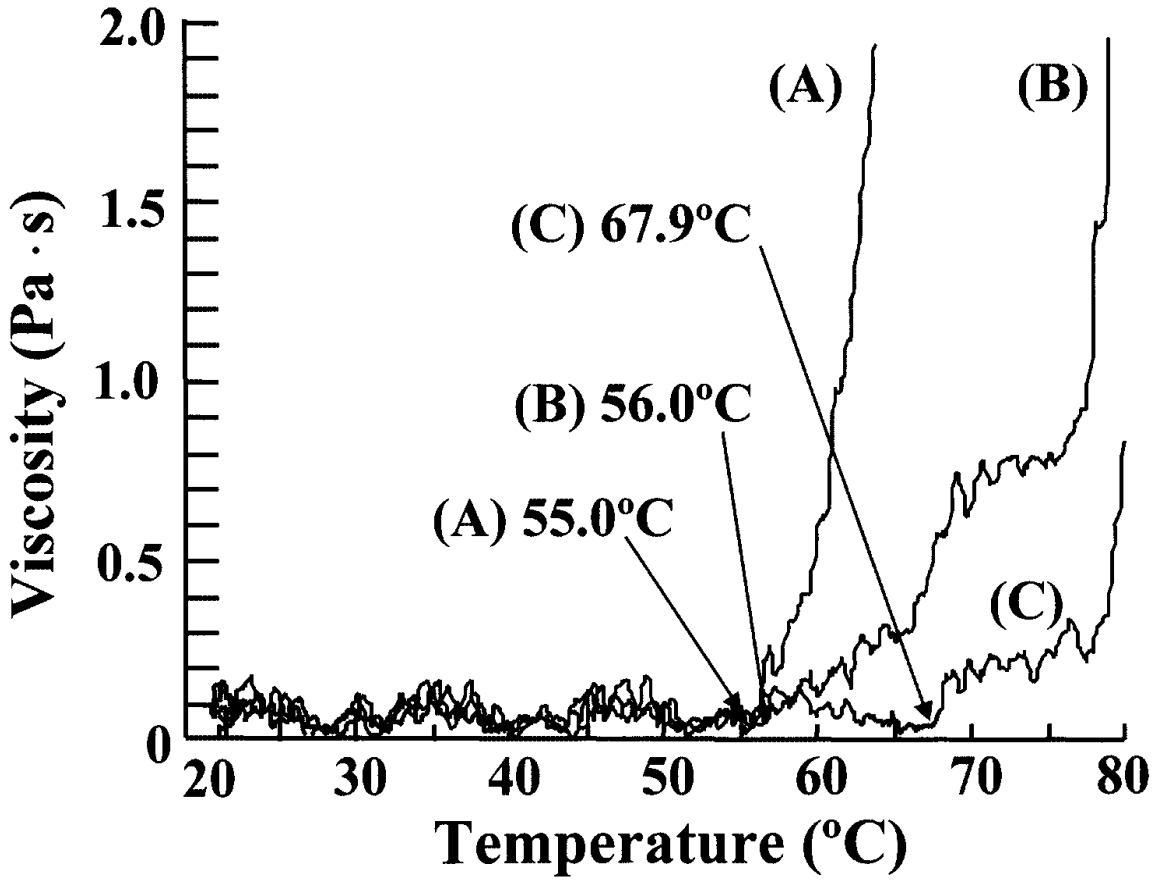

Figure 13: Effect of Nicotinamide on viscosity of aqueous HPMC-Nicotinamide solution with increasing temperature. As the concentration of Nicotinamide increases, (A) 0w/v% (B) 1.5w/v% (C) 3.0w/v%, the viscosity of HPMC decreases. The temperatures denote the gelation temperature.[37] Reprinted with permission from Elsevier. Copyright 2001.

While polymer viscosity plays a large role in varying release rates, polymer proportions can also play a role in the release profile from a matrix device. Increasing polymer proportion increases the gel viscosity which increases the diffusional path length. This increase in diffusional path length will then decrease the diffusion coefficient of the solute thus decreasing the drug release rate.[20] For example, a study of drug dissolution from select polymers found that changing the Methocel™ level from 10% to

40% led to a significant reduction in drug release rate while increasing the Methocel™ level resulted in an increased release rate.[20,38]

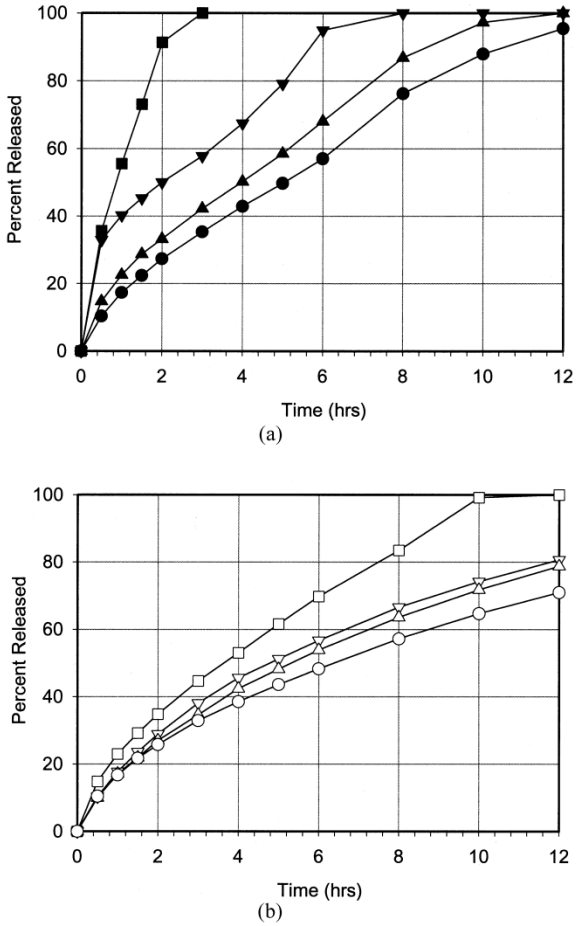

Figure 14: Effect of varying Methocel proportions on drug release. 10% Methocel (a) releases drugs at a faster rate than 40% Methocel (b) formulations. This is likely due to the effect of Methocel on the viscosity of the release polymer.[38] Reprinted with permission from Elsevier. Copyright 1998.

With viscosity playing a large role in the release rate of drugs from various polymers, individual particle properties undoubtedly play a role in drug kinetics. The number of particles in the polymer is directly proportional to the accessibility of particle contact points, viscosity, porosity and tortuosity of a given polymer matrix.[20] Furthermore, increasing the bulk density of a matrix exponentially decreases the rate at

which medium can penetrate the polymer's matrix network suggesting that increasing bulk density or decreasing porosity increases hydration resistance.[20,39] In addition to affecting the rate of hydration, increasing the particle size of HPMC have shown a

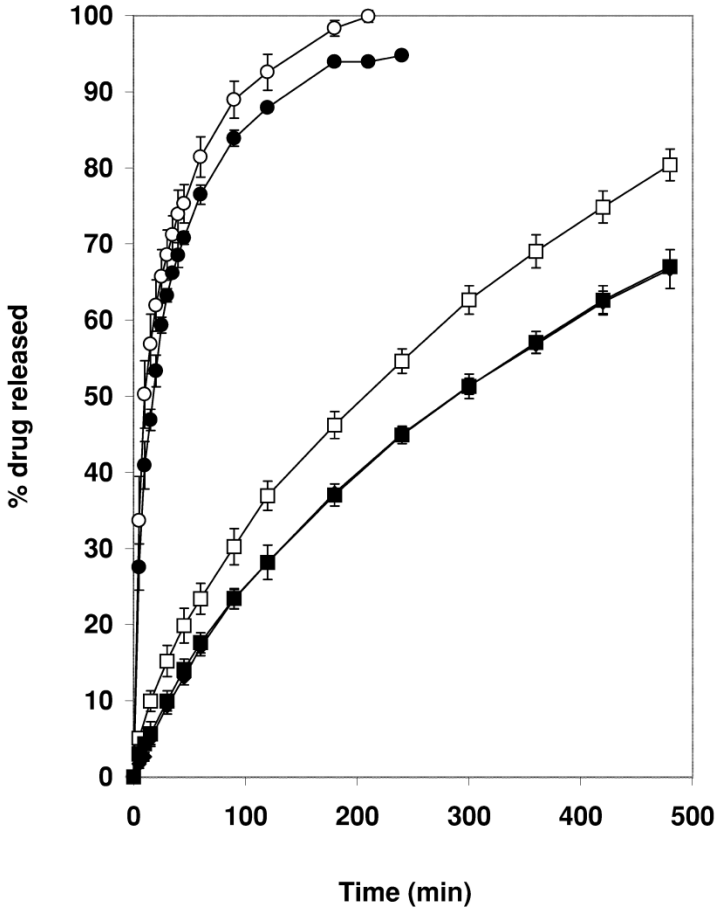

Figure 15: HPMC particle size affects rate of aspirin release from HPMC matrix. The rate of drug release increases with increasing particle size, 160-200µm (open circle), 100-120µm (closed circle), 70-80µm (open square), 40-50µm (closed square).[40] Reprinted with permission from Elsevier. Copyright 2001.

decrease in the lag period. This indicates a burst release of drugs before a gel layer develops at the polymer medium boundary layer. In Figure 15, Heng et al. shows the effect of particle size on the rate of aspirin dissolution from HPMC matrices.[20,40]

Using the data obtained from this experiment, Heng et al. developed Equation 6, a linear relationship ($R^2 = 0.9698$), to describe the effect of polymer particle size and number on the drug release constant (K_1).[20,40]

$$K_1 = \frac{D}{(N_{polymer}P_{polymer})^{1/3}} + A \qquad \text{[Equation 6]}$$

Where:

$N_{polymer}$ is the relative number of polymer particles in the matrix

$P_{polymer}$ is the mean particle size in the matrix powder

D is a constant representing matrix system's sensitivity to changes in $N_{polymer}$ and $P_{polymer}$

A is a release retarding constant

The final important polymer variable to consider is the combination of polymers. Recent studies have indicated gel layer consistency playing a role in the drug release kinetics.[20,41–43] Gel layer consistency is related to the rheological properties of the gelling agent or polymer. Rheologic synergism has been shown to enhance the rate of drug release due to favorable molecular interactions between polymers.[20]

2.3 Formulation Variables

An important formulation variable that can significantly affect the drug release profile of a controlled drug delivery system is system geometry.[20] Geometry can affect the rate of drug dissolution by altering the consistency and formation of the gel layer. The thickness of the gel layer is dependent on the available surface area of the drug delivery system. For example, the total drug release from a matrix with a planar surface is

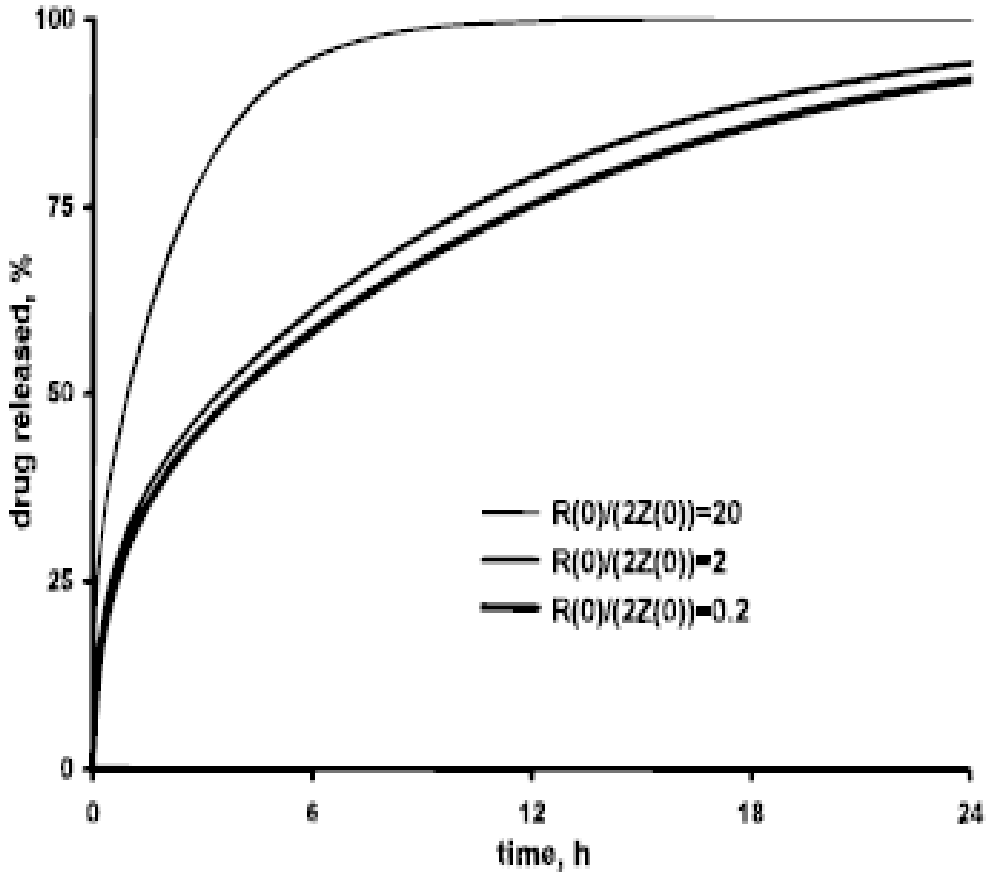

Figure 16: Effect of aspect ratio on drug release kinetics. As the aspect ratio increases, so does the drug release rate. A planar cylinder or disk (aspect ratio =20) is the fastest releasing system, next is a medium sized cylinder (aspect ratio = 2) and the slowest is a rod-shaped delivery device (aspect ratio=0.2).[29] Reprinted with permission from John Wiley and Sons. Copyright 1999.

proportional to the square root of time.[20] Other geometries will exhibit different kinetic profiles. Siepmann et al. examined the impact of aspect ratio (ratio of width to height) on drug release profiles.[29] Siepmann et al. found that increasing the aspect ratio, or increasing the planarity, of a drug delivery system resulted in quicker drug release kinetics.[29,44]

Chapter 3: Bio-MEMS in Drug Delivery

Microelectromechanical system devices, or MEMS, are micro-scale devices that have a distinct electrical or mechanical action.[45] Biomedical MEMS, or Bio-MEMS, are simply MEMS devices with biomedical applications.[45] Bio-MEMS can be used for a large number of physiological applications, including biosensing, drug delivery, microstructure support (stenting), tissue engineering.[45]

Bio-MEMS are usually fabricated through lithography.[46] Lithography involves cutting micro/nano-scale lines through sacrificial polymer coatings atop the desired substrate material. The polymer coatings are then removed through etching either with chemicals or light leaving behind a patterned substrate. The process is then repeated over multiple layers of sacrificial polymer layers and substrates until the desired design is obtained.[46]

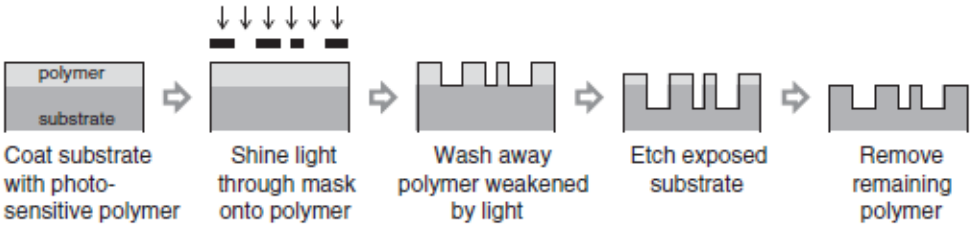

Figure 17: Overview of photolithography.[46] Reprinted with permission from Elsevier. Copyright 2013.

3.1 Microneedles

A large area of interest for BioMEMS drug delivery systems is transdermal delivery of drugs.[46] Drugs that are taken orally often are destroyed by the gastrointestinal tract, pass through unabsorbed or are rapidly absorbed and metabolized by the liver. Drugs that are susceptible to these disadvantages are often injected directly into the patient with a needle, however, needles are generally an unpopular alternative.[47,48] Microneedles, however, provide the opportunity for painless and efficacious drug delivery. The skin's transport barrier, the stratum corneum sits 20-50 μm from the surface of the skin, while the nerves are usually a few hundred microns below the surface of the skin.[49] Furthermore, the skin represents a more attractive target for vaccine delivery due

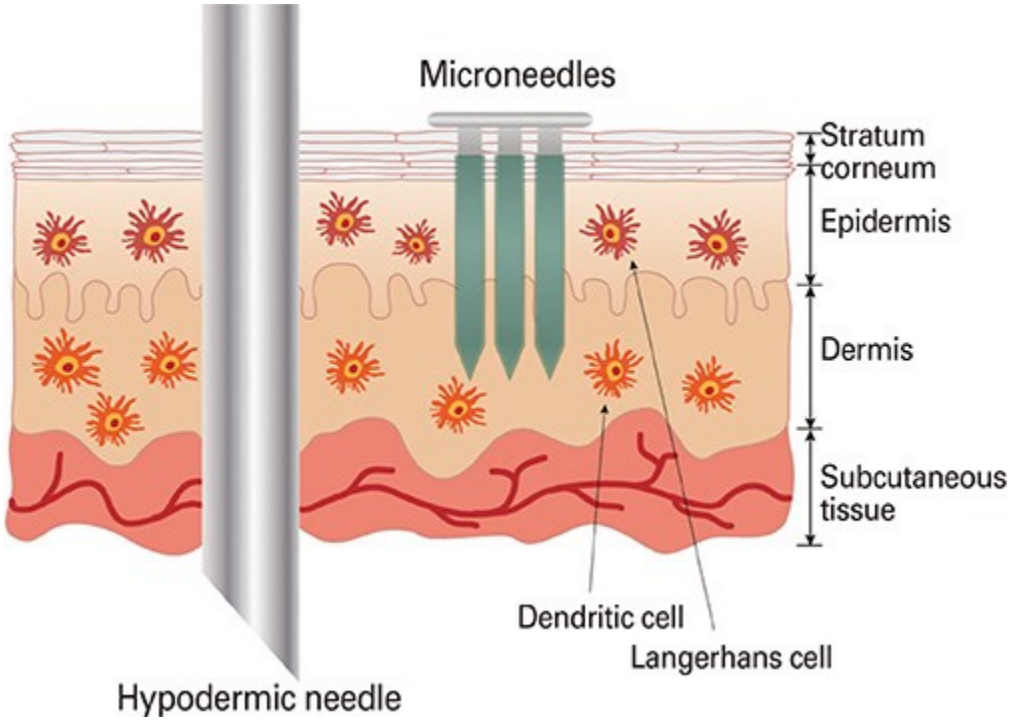

Figure 18: Microneedle vs. Hypodermic needle. The microneedles can sit high enough to avoid pain sensation, but also penetrate low enough to allow for effective delivery of therapeutic agents.[173] Copyright 2014.

to its highly immunoactive property.[50,51] There are several approaches to fabricate a wide array of narrow, sharp microneedles.[46,52–57] Most fabrication procedures involve photolithography to etch silicon substrate with either plasma (dry etching) or with a strong acid/base (wet etching). These processes allow for the fabrication of both hollow and solid microneedle arrays in a multitude of geometric formulations.[46,58–61]

Solid microneedles are conceived to be used a pretreatment step to puncture the stratum corneum. Then therapeutic agents can be applied to the skin and easily diffuse through the holes created by the solid microneedles. This technique was first exhibited *in vitro* fifteen years ago and was then rapidly translated to deliver insulin and genetic vaccines *in vivo*.[46,58,62,63] Recently, this technique is being used with human patients and

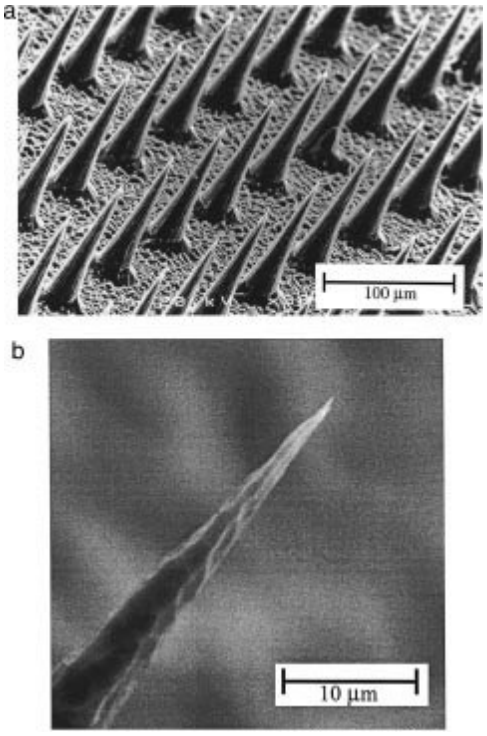

Figure 19: Scanning Electron Microscope images of microneedles. (a) A sample of 20x20 array of microneedles . (b) A zoomed in view of the microneedle tip.[58] Reprinted with permission from John Wiley and Sons. Copyright 1998.

will soon incorporate more complicated therapeutic agents such as elastic liposomes and prodrugs to increase the delivery and slow down natural healing of the holes created by the microneedles.[46,64–67]A particular challenge is to keep the pretreated pores open for an extended period of time so that the drugs can properly diffuse through the skin layer. Studies have found that microchannels will close within a few hours without any intervention.[68–70] With increasing research in the field of solid microneedles, there has been a shift towards finding new ways to utilize the technology for biomedicine. Studies have found that microporation created by solid microneedles can lead to an increase collagen regeneration in the skin which has led to the commercial release of a steel microneedle roller, called Dermaroller ®, in 2004.[71,72]

Coated microneedles take the concept of solid microneedles one step further. By coating solid microneedles with the therapeutic agent, the drugs are delivered directly into the micropores formed by the device.[73,74] A unique challenge to this approach is that the dose that can be administered each time is limited to the surface area of each microneedle surface; thus this method is restricted to sub-milligram doses.[73] Projects have focused on developing shapes and patterns that can maximize the surface area of the microneedles. Some common patterns and shapes are arrow-heads, sawteeth, slots and pockets that are fabricated into the needle shaft.[46,75–78] In addition to altering the pattern and shape of the microneedles, there has been a shift into developing novel coating formulations so as to maximize the loading potential, protect the therapeutic agent, and enhance the dissolution. Many polymer, polysaccharide and gum formulations have been studied and tested for this purpose.[46,73,76] In addition to engineering new coats, there has

been focus on also developing effective ways to apply the coat to the microneedles. Some explored techniques include painting, spraying, and immersion. Layer-by-layer techniques have become increasingly popular because of the ability to precisely control the coat thickness and area.[79,80] Dose controlling, however, becomes a more prominent challenge when attempting layer-by-layer deposition. The drug coated will be delivered more rapidly to the needles that to the base of the array. If done properly, however, it is possible to take advantage of this phenomenon to develop a dual-mode delivery system.[46]

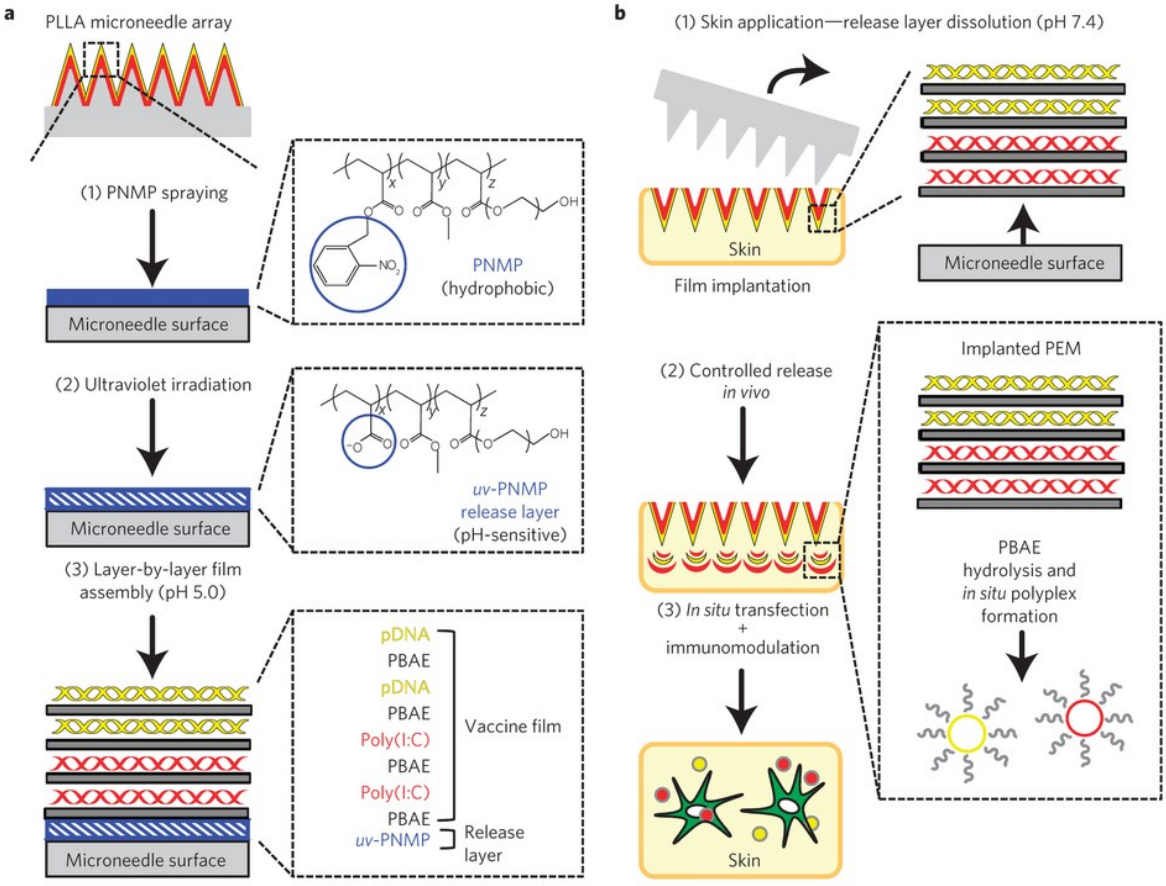

Figure 20: Coated microneedle layer-by-layer fabrication process. The coated microneedle pattern is first micropatterned onto a substrate. That substrate is then deposited with the therapeutic agent via layer-by-layer film deposition to allow for controlled release *in vivo*.[174] Reprinted with permission from Nature Publishing Group. Copyright 2013.

Another fabrication method includes creating porous microneedles with the active agent inside the needle shaft and then allowing it to diffuse out after penetration. Lastly, the tip of the needles could be fabricated out of a degradable polymer coating that is then detached and left in the skin as demonstrated in Figure 20. Passive diffusion using coated microneedles is an attractive therapeutic options because it allows for slow diffusion of the active agent. It has been used to deliver hormones, vaccines, adjuvants, DNA and live viruses.[46,81–92] A particular challenge with bioactive agents such as the ones listed is developing a method to maintain the stability of the agents over a long period of time especially when subjected to the physical and chemical constraints of the microneedle arrays.[93]

Solid microneedles are limited by the diffusion rate of the drug and the resealing of pores created in the skin; coated microneedles are limited by the complicated fabrication process and the difficulty for long-term storage. Hollow microneedles can potentially delivery large doses of liquid therapeutic agent via infusion, similar to conventional hypodermic needles.[46] Hollow microneedles avoid the challenge of diffusion limits and storage issues, however, present their own challenge through a more complicated fabrication process that involves intricate geometries. In particular, hollow needles channels weaken the shaft structure and increase the danger of breaking off while embedded in the skin. Furthermore, there is a need to develop a method for control to close the needle shaft opening so as to prevent the drug from leaking out until ready for delivery. Simultaneously, the shaft geometry and size must be such that the channel is not plugged up by the tissue that it penetrates but must be sharp and strong enough so that the microneedle can penetrate the dermis and stratum corneum to reach a pharmaceutically

and biological active site of the skin anatomy.[46] While these challenges are associated with the engineering and fabrication of the microneedle, some of the problems can be avoided logistically. Developing a rigid insertion protocol or adding accessories like

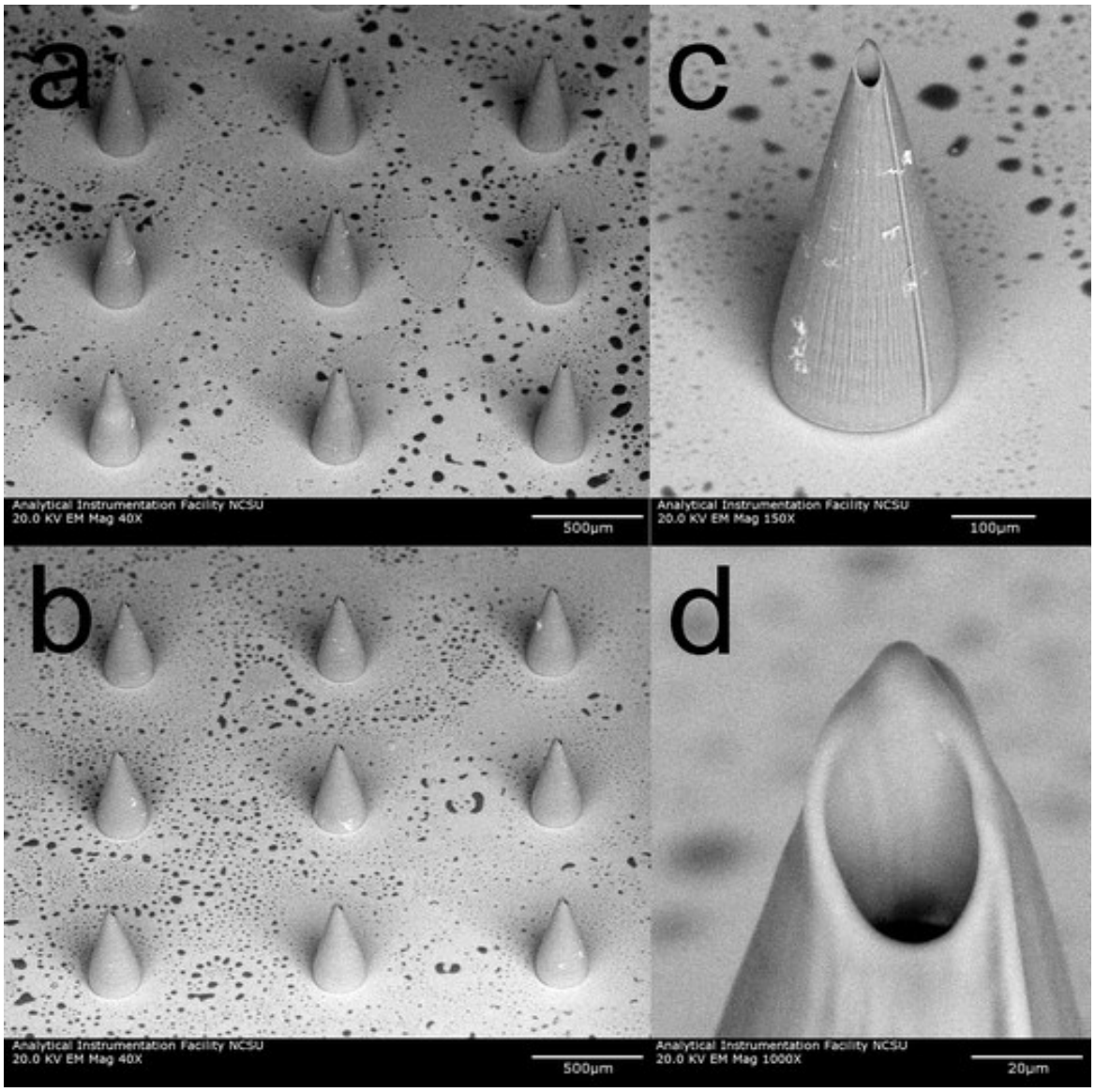

Figure 21: Scanning electron microscopy angled image of hollow microneedles. The image is obtained at 45° angle. (a) Image of 614 ± 12 µm long array of microneedles. (b) Image of 710 ± 10 µm long microneedle array. (c) Image of 710 ± 10 µm microneedle. (d) Zoomed image of 710 ± 10 µm individual microneedle. The base diameter of the microneedles is 226 ± 5µm.[175] Reprinted with permission from The Royal Society of Chemistry. Copyright 2011.

electronic impactors and vibrating actuators can allow for reliable insertion of hollow microneedles without damaging or clogging the needle.[46,94–98] Hollow microneedles were first built in two-dimensional arrays and had the shaft running parallel to substrate layer from which it was formed.[99] This fabrication pattern limited the number of microneedles that could be fabricated in each array but made it easier to include extra patterns such as barbed tips, microfilters inside the base of the needle shaft, nanofilters inside the tip of each microneedle and even small pockets that allow for gas lift to precisely control the infusion of the liquid therapeutic agent.[46,100–104] Three-dimensional microneedle arrays contain simpler patterns but allow for a larger subset of possible geometries that have been examined and tested. Potential geometries include "blunt cylinders, beveled

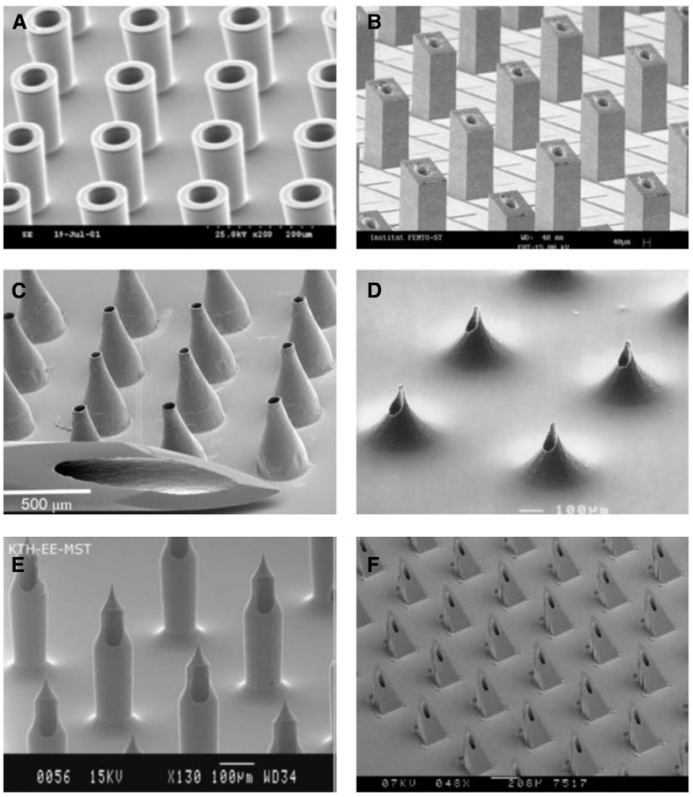

Figure 22: Micrographs of hollow cylinder microneedle geometries. (A) Blunt cylinders. (B) Beveled columns. (C) Metal Conical. (D) Off-centered volcano style (E) Citadel-style. (F) Sawtooth-style.[46,59,105–109] Reprinted with permission from Elsevier. Panels A, B: reprinted with permission from Springer. Panels C-F: Reprinted with permission from IEEE Copyright (2005, 2005, 2007, 2003)

columns, metal cones, volcano-shaped microneedles with channels on the slope of the peaks, sawtooth microneedles, and citadel-shaped microneedles opening at the sides of the shaft to avoid coring."[46,59,105–109] Some needles can cover the opening of the shaft with a gold cap to keep the liquid therapeutic agent within the microneedles and prevent premature leakage. When the microneedles is pushed up against the skin's surface, the gold cap ruptures and allows for the unhindered infusion of the fluidic drug.[110] Recently, a variety of hollow microneedles have entered and completed the FDA clinical trials for a multitude of applications including, insulin pumping, rabies vaccination, polio vaccination, and glucagon injections.[46,111–117]

Microneedles have also been used for both ocular and nasal drug delivery.[46,118,119] The microneedle has been added to some vascular stents and vascular wraps to administer drugs that will prevent restenosis of the vascular wall.[46,120,121] Microneedles have also been added to other drug delivery strategies such as iontophoresis and electroporation.[46,122–126] Overall, microneedles are a unique and important field of bio-MEMS drug delivery and have a bright future. New studies and integration of external novel concepts will allow the biomedical and medical community realize the potential of the microneedles for drug delivery. More importantly, advances in microfabrication techniques for precision, accuracy and control will allow for large-scale generation of highly efficacious drug delivery systems to allow for painless, hassle-free insertion of drugs via dermal and subcutaneous pathways.

3.2 Polymer/Hydrogel Gastrointestinal Patches

Many drugs require oral delivery rather than intravenous or intramuscular injection. There are a large number of drugs and doses that limit the universality of microneedle based drug delivery. Furthermore, oral drug delivery does offer the advantage of increasing patient compliance and patient safety.[127,128] There is a shift towards developing novel "peptide, protein, biopolymer and macromolecular [based] drugs for treatment of a variety of diseases."[127] Unfortunately, these drugs, when administered orally, will often fail to achieve the desired clinical response. This is due to multiple factors, "including: (i) a low mucosal permeability of a drug; (ii) the permeability of a drug being restricted to a particular region of the gastrointestinal (GI) tract; (iii) the low solubility of a compound, resulting in a low dissolution rate in mucosal fluids; and (iv) a drug being unstable in the GI environment, resulting in its degradation before absorption."[127,129] The most important limiting factor for oral bioavailability of these drugs is "luminal enzymatic hydrolysis and low membrane permeability."[127,130] Overall, in order to increase the oral bioavailability of these drugs, they must overcome the harsh environment of the multitude GI compartments and must maintain a long residence time in the GI tract. To create systems that can survive the stomach, there have been attempts to create microspheres and nanoparticles with protective coatings made from lipids or other polymers, similar to encapsulation. These systems offer a unique method to pass through the stomach and also increase the transport of the drugs through the intestinal walls.[127,131–135] In addition to protective coatings, in order to increase residence time in the GI tract, several systems have been tested including, magnetic systems, gastric retentive units and polymers with particularly strong mucoadhesive

properties.[127,136–143] Furthermore, there have been studies that have examined the efficiency of non-specific mucoadhesive polymers and cytoadhesive agents to target specific sites in the small intestine.[127,129,144–146] All of these advancement are promising when it comes to delivering large molecules, however, none of them have been proven to be a solution for safe oral administration.[127]

A proposed solution to the problems of oral drug delivery is developing a multilayered patch device that is similar to transdermal patches, such as nicotine or contraceptive patches.[127,147–149] These patches "comprise layers of thin, flexible membranes; an impermeable backing; a drug reservoir; a rate-controlling membrane; and an adhesive."[127] When attached to the desired substrate, skin or GI wall, the membrane will regulate the rate of drug delivery to keep the drug within the therapeutic window. There has been some recent success with these buccal patch devices for drug delivery via the oral mucosa.[127,150–153]

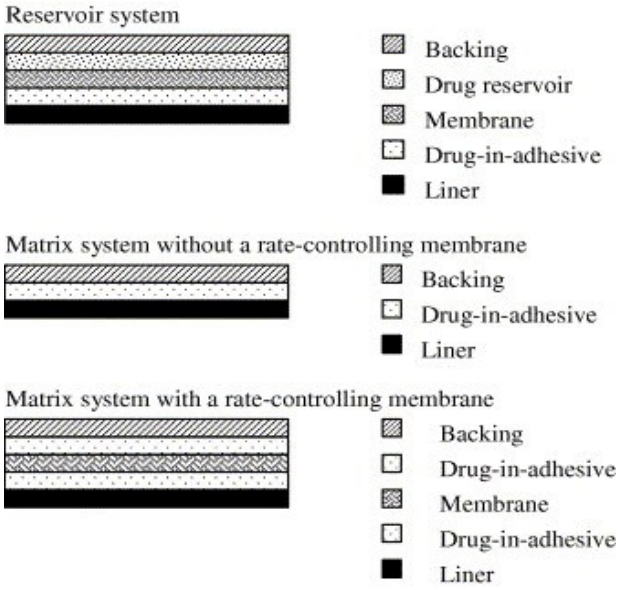

Figure 23: Three types of drug delivery patches. Each combination will result in a different drug delivery kinetics and dosing.[176] Reprinted with permission from Elsevier. Copyright 2006.

The first GI patch for oral drug delivery was the GI-mucoadhesive patch system (GI-MAPS) developed by Eaimtrakarn et al.[130,154] The patch contained "four layers: (i) a backing layer made of a water-insoluble polymer to protect protein drugs from enzymatic hydrolysis; (ii) a surface layer made of a polymer sensitive to intestinal pH; (iii) a drug-carrying middle layer; and (iv) an adhesive layer between the middle and surface layers to generate a high concentration gradient between the patch and intestinal enterocytes."[127]

Figure 24: Capsule with GIMAPS.[127] Reprinted with permission from Elsevier. Copyright 2005.

The group inserted the patches intradudoenally, to bypass the stomach, and test the mucoadhesion while tracking the location of the patch system through the GI tracts of fasted male Wistar rats.[130] They also tested the patches sensitivity to varying pH throughout the different locales of the GI system. They tested three different pH-sensitive polymers, HP-55, Eudragit® L100 and Euragit® S100, as the surface layer of the GI-

MAPS which resulted in delivery of drugs to different locations in the small intestine. They observed a correspondence between pH levels at different locales of the intestine with the threshold of the pH-sensitive polymers. The pH-sensitive polymers degraded at their pH threshold leaving behind the mucoadhesive layer which would then interact with the mucosa of the small intestine and be captured. In this experiment, the group tested pH values ranging from 6.6 to 7.5 in the duodenum/jejunum and ileum respectively.[127,130,154] They discovered that the HP-55 patches had a pH-threshold of pH 5.5 and mostly located to the duodenum; the Eudragit® L100 patches had a dissolution threshold of pH 6.0 and mostly stuck to the jejunum mucosa; and the Eudragit® S100 patches dissolved at pH 6.8 and were retained in the distal ileum.[127,130,154] The group then tested each polymer patches' efficiency at targeting particular locations of the small intestine in male beagle dogs. To model drug release, the group loaded the patches with 30mg of fluorescein and monitored the plasma fluorescein levels. After this study, they found that HP-55 and Eudragit® L100 patches reached peak fluorescein levels at 2.3 and 3.3 hours, respectively, while Eudragit® S100 patches delayed the release by 2.3 hours and then reached peak leavels 5 hours after insertion.[127,130,154] Lastly, the group tested the patches' ability to release recombinant human G-CSF. The group loaded the GI-MAPS with 125μg of recombinant human G-CSF and then monitored white blood cell counts. The pharmacological availability of G-CSF when delivered via GI-MAPS was 5.5% for HP-55 patches, 23.0% for Eudragit® L100 patches and 6.0% for Eudragit® S100 patches. They hypothesized that the Eudragit® L100 patches resulted in the highest pharmacological availability because the hydrolytic enzyme activity and intestinal content is lowest in the jejunum where the Eudragit® L100 patches located. For delivery

of recombinant human G-CSF, the Eudragit® L100 patches outperformed its GI-MAPS counterparts, other colonic delivery systems and enteric effervescent systems.[127,155,156]

To further improve on GI patches, Eaimtrakarn et al. set out to develop a patch with increased drug loading space by removing the mucoadhesive layer, termed drug-in-adhesive patches.[157,158] The new patch contained "three layers: (i) a backing layer of ethylcellulose; (ii) an enteric polymer membrane of HP-55; and (iii) a new drug-carrying layer, based on Carbopol®, loaded with 30 mg of fluorescein or fluorescein-dextran as a model drug."[127] Each patch loaded with 30 mg of fluorescein was comparable to a compressed fluorescein tablet that contains 30 mg of dye. The group tested the patches' ability to elute drugs *in vitro* by placing the patches in phosphate buffer pH 7.4 at 37°C. They found that the patches eluted the first 50% of fluorescein two times slower than the tablet confirming the sustained release characteristics of the patches. *In vivo* studies in beagle dogs with fluorescein loaded patches resulted in a "mean residence time of

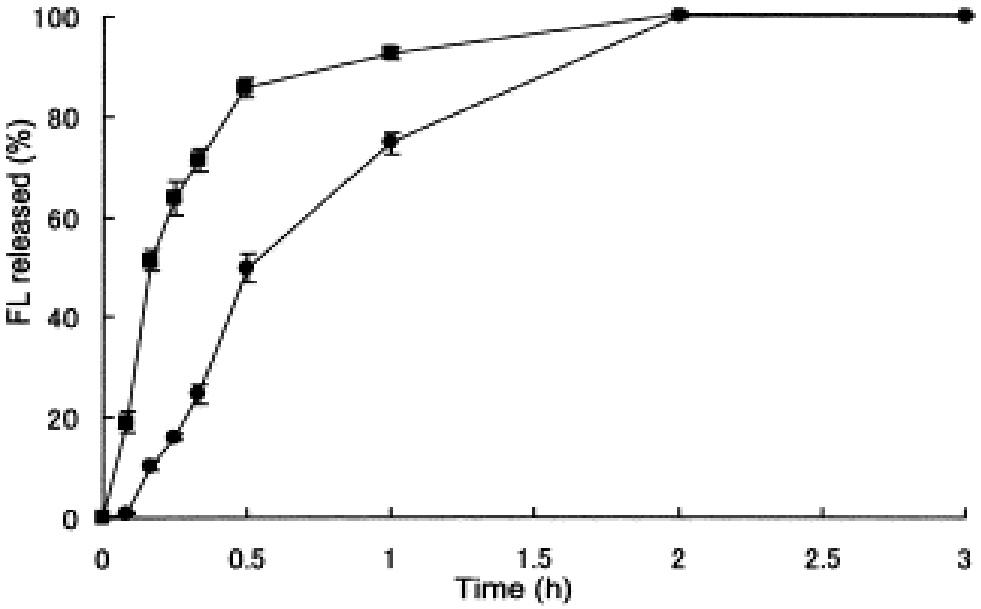

Figure 25: Dissolution of fluorescein from patches (circles) and tablets (squares).[157]
Reprinted with permission from Elsevier. Copyright 2003.

fluorescein in plasma…1.5 times greater than tablet preparations."[127]

The group also tested the drug-in-adhesive patches in human volunteers by observing the release of caffeine as the model drug. They loaded the patches with 50 mg of caffeine and administered 120 patches by enteric encapsulation. Both fasted and fed human volunteers were administered the drug-in-adhesive patches and the group monitored caffeine release by examining salivary caffeine excretion. Eaimtrakarn et al. also established a control by examining the immediate release of caffeine in fasted individuals which produced a mean maximum caffeine excretion rate of 2μg/min at four hours.[127] The drug-in-adhesive patches under fasted conditions exhibited a mean maximum excretion rate of 1.75μg/min at six hours which is a lower mean maximum

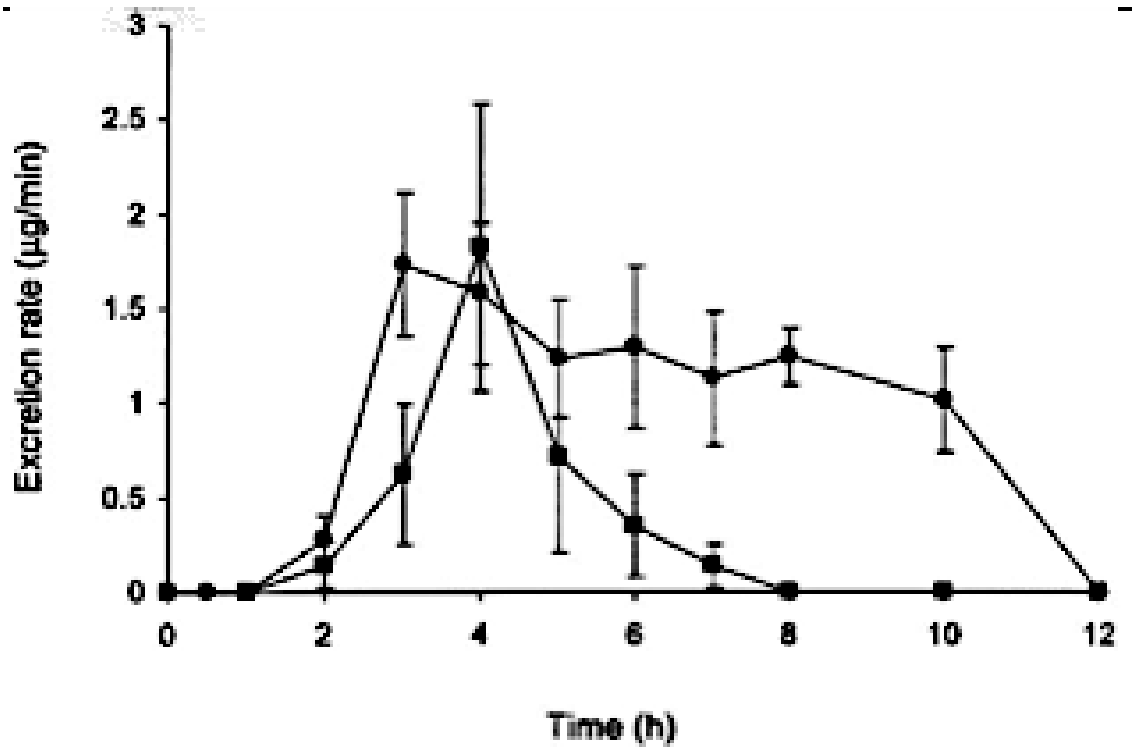

Figure 26: Salivary caffeine excretion rate vs. time under fasted conditions. The enteric capsules containing caffeine (square) has a lower residence time than the caffeine patch system (circle).[158] Reprinted with permission from Elsevier. Copyright 2002.

excretion rate than the control but a higher residence time. In the fed human volunteers, the control and patch systems had similar kinetic release rate with caffeine appearing the saliva two to three hours after administration. This indicated that the presence of food extended the gastric emptying time of the capsules containing the patches. The group concluded that the patches resulted in a longer mean residence time of caffeine in the small intestine under both fasted and fed conditions.[158]

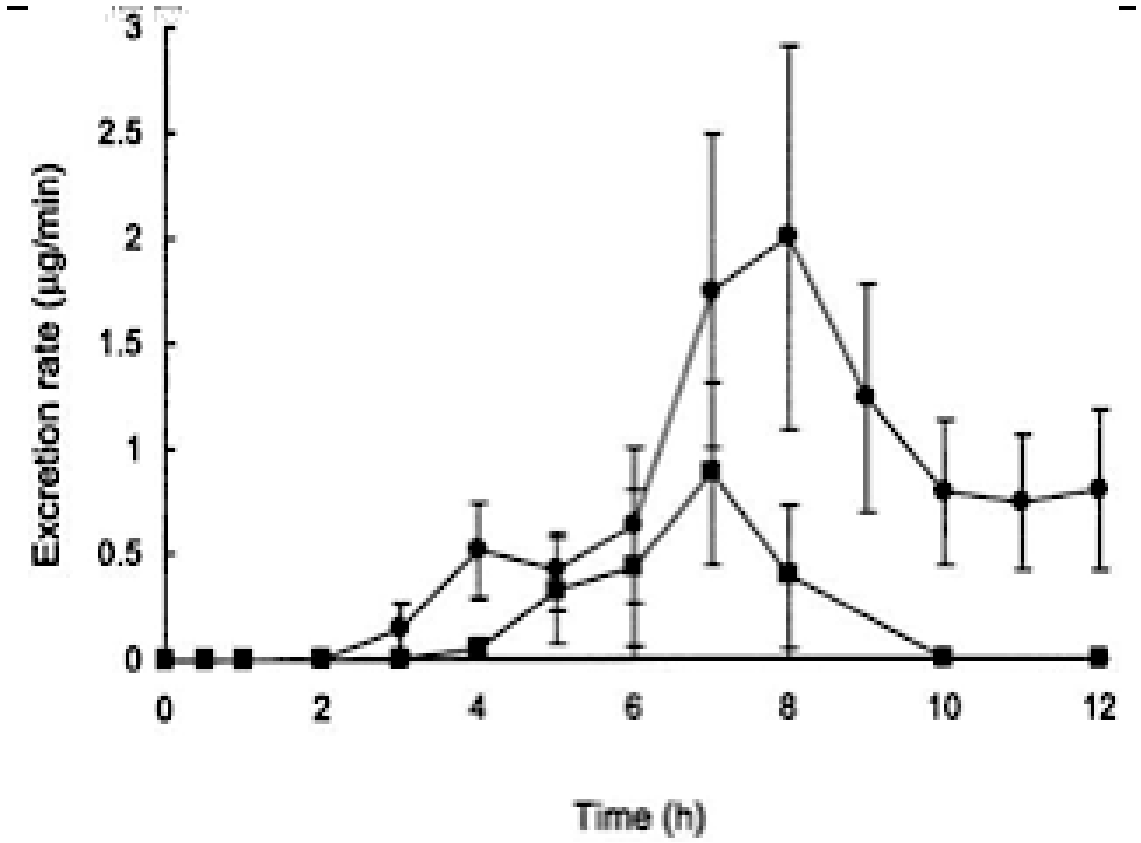

Figure 27: Salivary caffeine excretion rate vs. time under fed conditions. The enteric capsules containing caffeine (square) has a lower residence time and lower mean maximum salivary excretion rate than the caffeine patch system (circle).[158] Reprinted with permission from Elsevier. Copyright 2002.

In addition to GI-MAPS, and drug-in-adhesive patches, Shen et al. developed an alternative patch system that contains three layers: "(i) a mucoadhesive layer; (ii) a layer of drug-loaded microspheres partially immersed in the mucoadhesive layer; and (iii) an impermeable membrane encompassing the microspheres."[127]

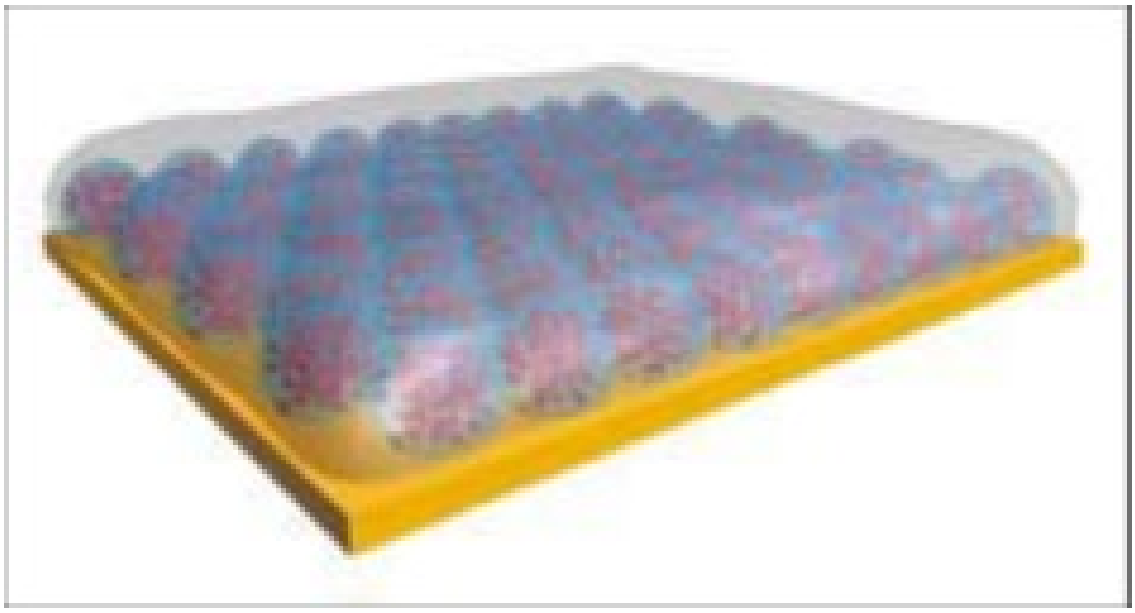

Figure 28: Design for microsphere GI drug delivery patch.[127] Reprinted with permission from Elsevier. Copyright 2005.

Shen et al. fabricated the patches by cross-linking bovine serum albumin (BSA) microspheres 10-30 microns in diameter and loading them with one of the three model drugs, sulforhodamine B, phenol red, or fluorescein isothiocyanate (FITC)-dextran. They then uniformly dispersed the microspheres into a five-micron thick Carbopol® and pectin mucoadhesive layer. The mucoadhesive layer was then covered with an ethylcellulose layer. The group then tested the release of sulforhodamine B from four millimeter patches *in vitro* by immesersing the patches in phosphate buffered saline (PBS). They discovered

that the 95% of the drug released from the side that contained the mucoadhesive layer. Shen et al. then tested the patches *ex vivo* across an explanted Sprague Dawley rat intestine section. The explanted intestine section with the patches attached to the surface were then immersed and infused with PBS with a flow rate of 0.05 ml/min. The group then monitored the concentration of drugs in the exiting PBS. The control was determined by injecting the same quantity of drug directly into the into the intestinal lumen. All three model drugs were found to have enhanced transport across the intestinal wall when administered via the patch as compared to the control. The group determined

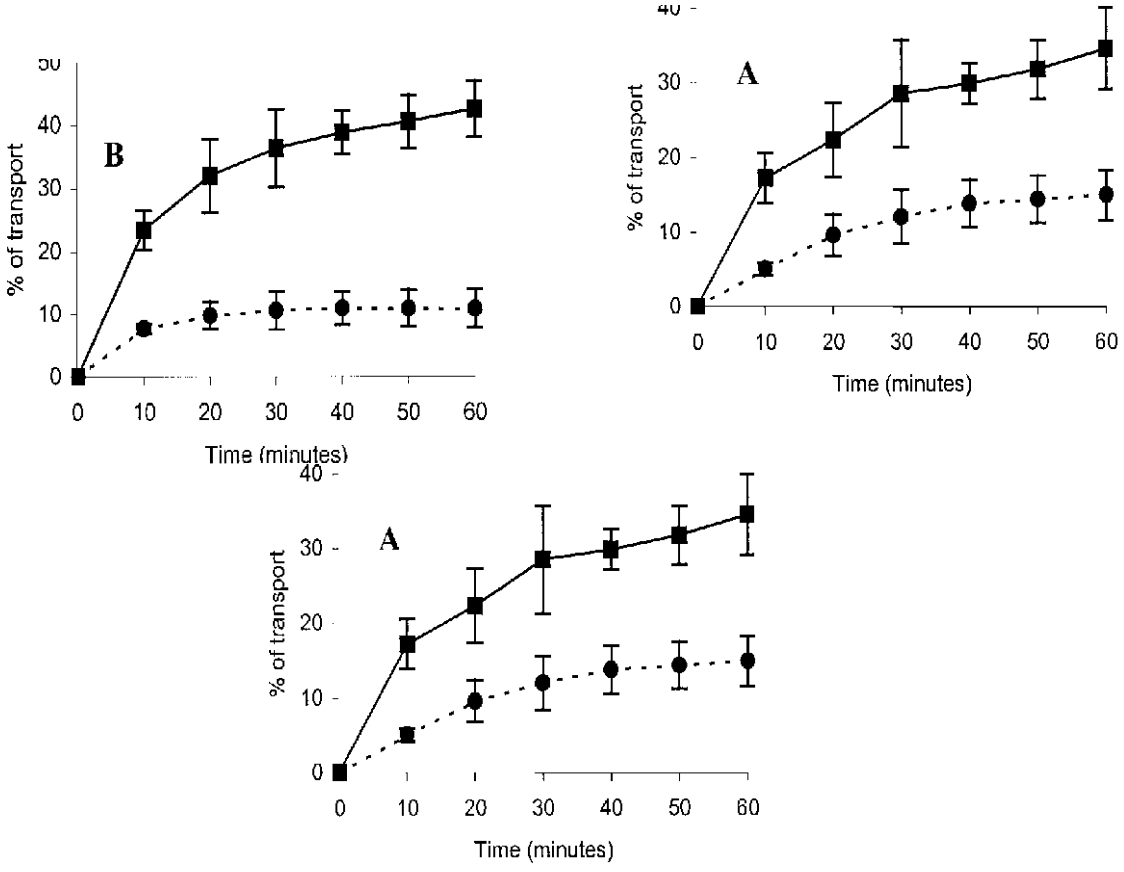

Figure 29: Release of model drugs from patch vs. control groups. In each graph the patch (square) shows greater drug release than the control (circle). (A) Sulforhodamine B. (B) Phenol red. (C) FITC-dextran.[159] Reprinted with permission from Springer. Copyright 2002.

the intestinal wall allowing for a higher concentration gradient which allows the patch to maintain unidirectional diffusion in a direction orthogonal to the intestinal wall.[127,159]

GI patches offer a unique ability to improve the efficacy for oral drug delivery, maintain a safe dosage and allow for controlled drug delivery. The systems are optimized and engineered to perform multiple functions using the same basic platform. The future of hydrogel patches are bright and future studies on how GI patches can be further developed to allow for more efficient and efficacious drug delivery. Moreover, the discovery and creation of new materials, in particular biocompatible and biodegradable hydrogels will allow for novel GI patches that can allow for more regulated and long-term drug release.

3.3 Self-Folding Drug Delivery Systems

Self-folding devices for controlled drug delivery have a bright future. Self-folding devices have been examined as potential microsurgical tools. In general, polymer based self-folding devices are fabricated by combining a swellable polymer bilayer to allow for the folding actuation. Through self-folding, the complicated two-dimensional structure can be turned into asymmetric three-dimensional structure with an increased number of possible mechanical actions.[46,160,161] For example, Figure 30 shows a six-panel two-dimensional cruciform shape that can spontaneously fold into a three-dimensional hollow cube that is 500 microns wide. The actuation component is added to the system

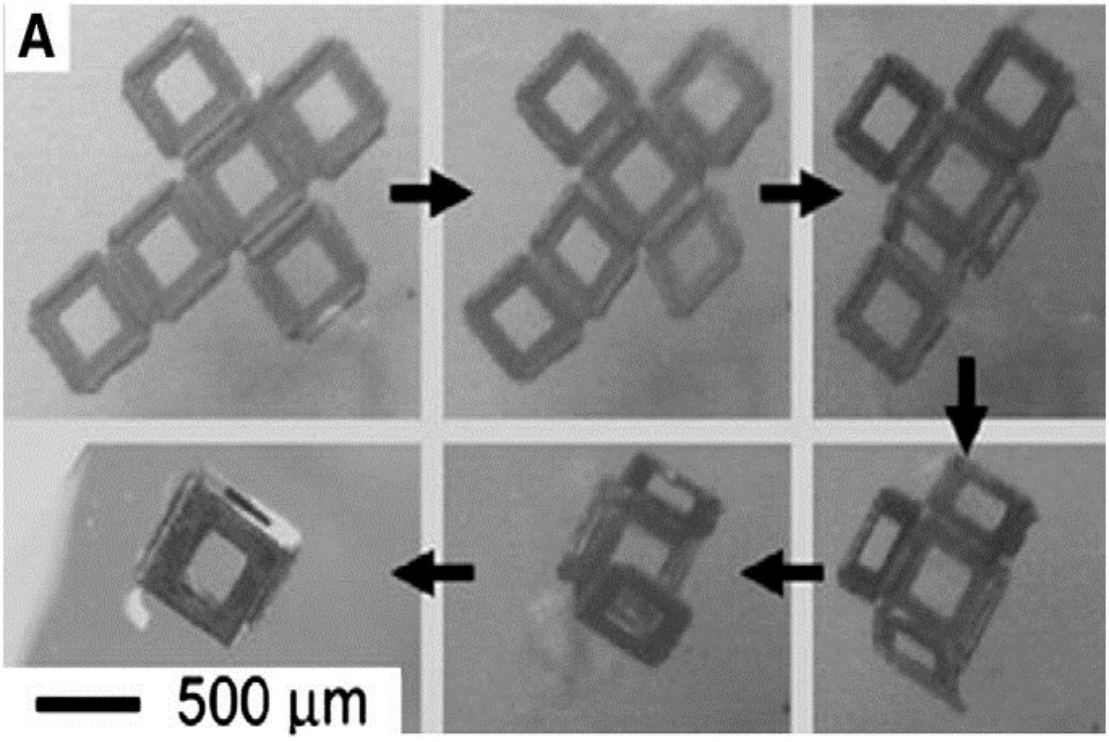

Figure 30: Self-folding two dimensional device that can spontaneously create a cube.[161] Reprinted with permission from Elsevier. Copyright 2007.

during the fabrication process of the two-dimensional device. Each panel is fabricated with a different functional element that leads to differential stresses on the overall frame and paneling in the structure.[46,160] The combination of differing stresses on each panel structure at specific time intervals, allows for the two-dimensional structure to fold into a three-dimensional cube.

Similar folding mechanisms can be developed with copolymer mixtures.[160] Boncheva et al. developed a method to demonstrate self-folding of two-dimensional planar sheets to create three-dimensional spherical shells using a polydimethylsiloxane (PDMS) shells and magnetic force. The group had to develop PDMS elastomers that are were embedded with magnetic dipoles. The self-folding shape configuration was mostly driven by the interaction between the elastic bending forces and the magnetic forces.[160,162] Randhawa et al. developed a microchemomechanical system (MCMS) that was composed of polymer triggers on stressed metallic thin films allowing for chemically actuated gripping devices. The MCMS devices were essentially wireless microsurgical tools that folded and unfolded upon exposure to enzymes like trypsin and cellulose.[163,164] In general, self-folding polymeric devices are mostly reliant on differentially stressed layers to allow for the creation of curved structures.[160]

Self-folding drug delivery devices allow for unidirectional release of loaded therapeutic agents.[160] He et al. developed a three-layered, polymer-based, mucoadhesive drug delivery system "consisted of a swelling layer, a non-swelling layer and a mucoadhesive (drug loaded) layer."[160,165] The group crosslinked with swelling layer with a pH-sensitive poly(methyl methacrylate) (PMMA)-based hydrogels. They also

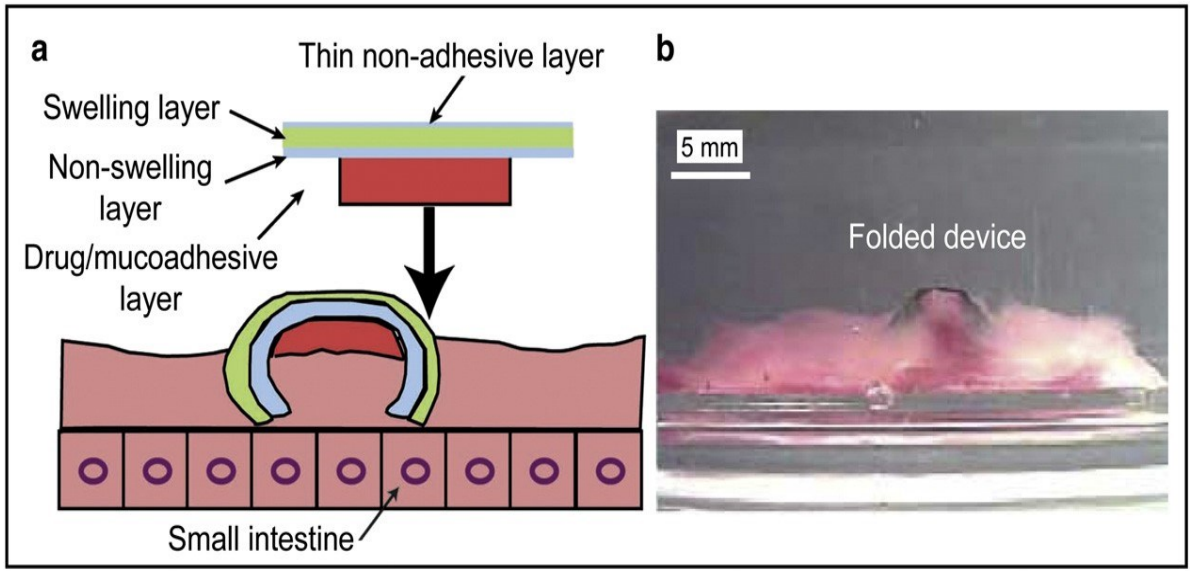

Figure 31: Three-layered, polymer-based, mucoadhesive self-folding drug delivery system. The system contains a swelling PMA hydrogel, a non-swelling PHEMA hydrogel and a drug loaded PVA/Carbopol® mucoadhesive layer. (A) Schematic of device in action. (B) Picture of the device in action on a explanted porcine small intestinal surface.[165] Reprinted with permission from Elsevier. Copyright 2006.

crosslinked the non-swelling layer with a poly(hydroxylethyl methacrylate) (PHEMA)-based hydrogel, which also acted a diffusion barrier. The mucoadhesive layer was composed of poly(vinyl alcohol) (PVA) and Carbopol® along with the therapeutic agent.[160,165] As exhibited in Figure 31, the mucoadhesive layer was in complete contact with the explanted small intestine. This ensured unidirectional release of the drugs into the small intestine. Furthermore, the PHEMA layer acted a diffusion barrier and thus the drug release from the device was lower than the control experiment.[160,165] The unidirectional, controllable release of the drug increases the drug's efficacy, reduces the

required dosage and also decreases the number of side effects.

Self-folding device also allows for spatio-temporal control of drug delivery. Kalinin et al. used computer simulations to demonstrate the release of chemical agents

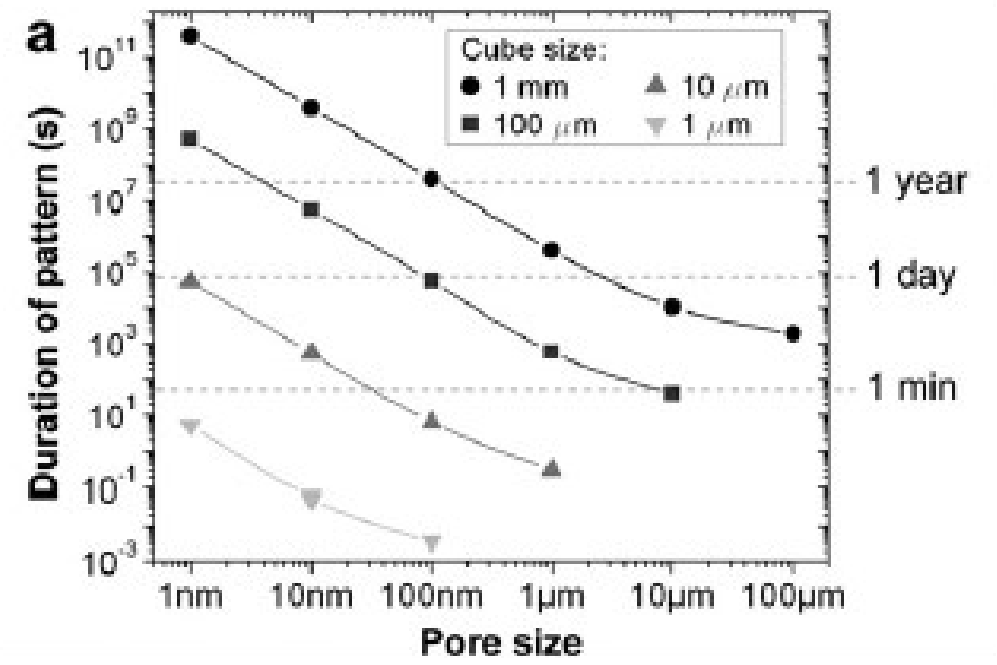

Figure 32: Spatio-temporal control release of polymer drug delivery device. Plot depicting the release of drug s in a few seconds to the life span of a human showing the relationship between cube size, pore size and the length of drug release form the device.[166] Reprinted with permission from John Wiley and Sons. Copyright 2011.

from "porous, self-folded cube over time-scales ranging from a fraction of a second to a human life-time by varying" the cube size and pore size.[160,166] They discovered that spatial control was dependent on the shape of the drug delivery device. Furthermore, controlling the pore diameter and thickness of the device wall allowed for temporal control of the drug.[160,166]

Recently, in 2014, Malachowski et al. developed a stimuli-responsive chemomechanically controlled gripper device termed theragippers. The grippers were

fabricated using alternating rigid panels of poly(propylene fumarate) (PPF), a biodegradable and photopatternable polymer, and flexible hinges of poly(*N*-isopropylacrylamide-*co*-acrylic acid) (pNIPAM-AAc). The pNIPAM allows for thermally responsive capability for the grippers to actuate at a temperature above 32ºC. The rigid PPF panels ensure that the grippers have sharp tips to penetrate the tissue. Lastly, the porous polymers allow for controlled release of therapeutic agents from the theragrippers. The group then tested the theragripper's ability to release mesalamine, an anti-inflammatory drug for inflammatory bowel disease (IBD), and fluorescein, a model drug. The group also tested the theragripper's mechanical attachment to tissue *in vitro* to model flow conditions that would be experienced in the GI tract. Overall, Malachowski et al. found that the polymer based theragrippers allow for absorption of drugs and slow controlled release of drugs over a period of a week.[167]

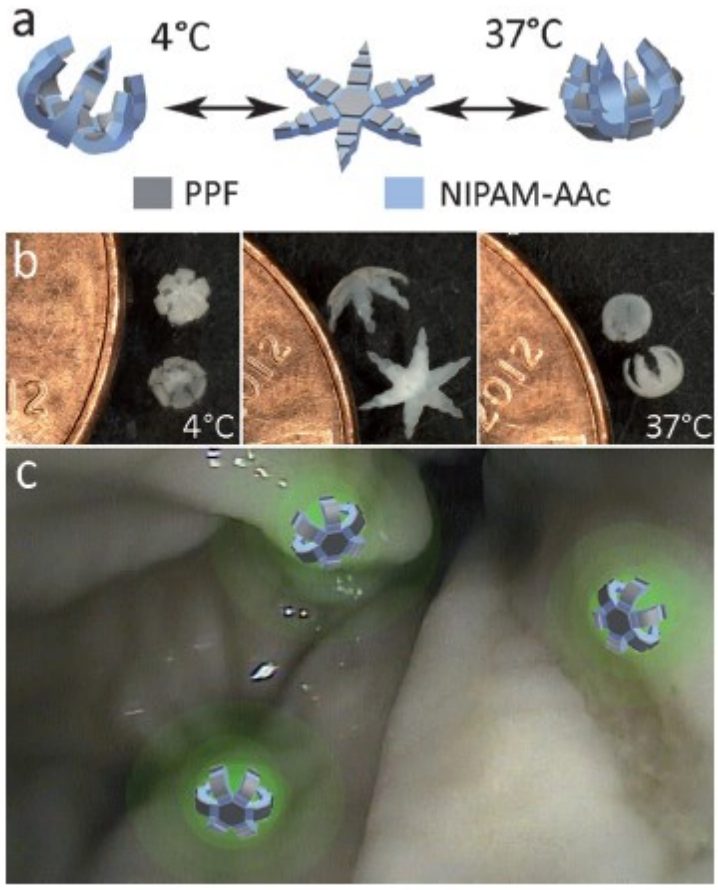

Figure 33: Schematic diagram and image of drug-eluting theragrippers. (A) Schematic of theragrippers fabricated with rigid PPF paneling and flexible stimuli-responsive pNIPAM hinges. (B) The threagrippers are closed at 4ºC and then open, flip, and close when exposed to 37ºC. (C) A conceptual depiction of the theragrippers attached to colonic wall releasing a fluorescent drug for spatio-temporally controlled drug delivery.[167] Reprinted with permission from John Wiley and Sons. Copyright 2014.

Chapter 4: Paraffin Wax for Drug Delivery

4.1 Introduction

With the recent development of microgrippers, metallic, tetherless, thermobiochemically actuated microsurgical tools, has opened up a variety of potential opportunities for biopsy and drug delivery. The microgripper actuation is based on a fabricated mechanical stress layer that allows for the device to fold.[164] Actuation can be dependent on temperature or chemical-stimuli. Paraffin wax is a material of particular

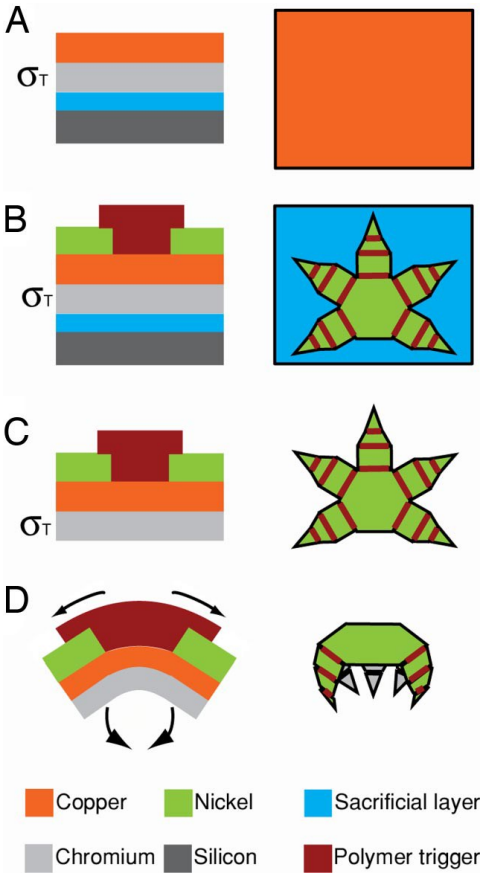

Figure 34: Schematic representation of side (left) and top (right) views of the fabrication process for microgrippers. (A) The bimetallic joints (orange and light gray) are thermally deposited over the sacrificial layer (blue) and silicon (dark gray). The chromium layer (light gray) will develop a tensile stress during thermal deposition. (B) The nickel paneling (green) and the polymer trigger layer (red) are patterned over the bimetallic layer. (C) The sacrificial layer is dissolved to remove the microgrippers from the silicon wafer. (D) When stimulated the polymer trigger layer softens allowing for the bimetallic layer to flex.[164]

interest for thermally-stimulated actuation. Figure 34 depicts the fabrication process for microgrippers. The polymer trigger layer can be any layer with enough mechanical strength to keep the gripper open until actuation. Polymer trigger layers of interest are those that can be specifically optimized to allow for actuation at predetermined temperatures and chemical stimuli.

Paraffin is a soft solid derived from petroleum, coal or oil shale. The material is a mixture of long hydrocarbon chains that contain between twenty and forty carbon atoms. It exhibits unique physical properties as well, with a melting temperature slightly above 37ºC and a boiling point above 370ºC.[168] Because of its melting temperature of 37ºC, paraffin wax is a great material choice for a polymer trigger layer since body temperature is 37ºC.

Figure 35: Paraffin wax.[177] © 2013 Googana Exports PVT. LTD.

4.2 Background

Historically, wax has been a material of interest for controlled drug release. Specifically, carnauba wax, a naturally occurring wax derived from the leaves of the palm *Coperinicia pruniferia* has been studied for potential drug delivery applications.

In 1993, Huang et al. examined an acrylic polymer-wax matrix system for sustained-release table for diphenhydramine hydrochloride (HCL). The group combined carnauba wax with Eudragit L-100®. The group used lactose as a filler to achieve the desirable tablet size. To examine the effect of carnauba wax and Eudragit L-100 on the release of drugs, Huang et al. studied the release of drugs in varying polymer-to-drug-to-wax ratios.[169]

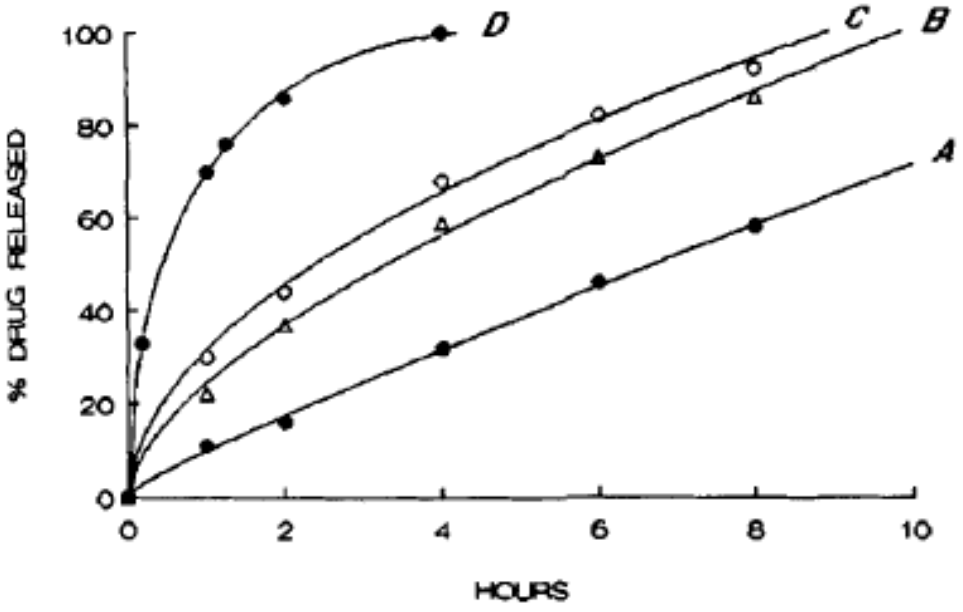

Figure 36: Effect of varying polymer, drug, and wax ratios on the release of drugs. Polymer:Drug:Wax Ratios - (A) 2:1:1. (B) 1:1:1. (C) 1:2:3. (D) 0:1:1.[169] Reprinted with permission from John Wiley and Sons © 1994.

As is depicted in Figure 36, formulation D, the formulation with only wax and drugs resulted in the fastest release of the drugs. This indicates that wax allows for some release of drugs, albeit mostly burst release. Formulations A, B, and C allow for the most sustainable long-term release of drugs.

Even earlier, in 1967, Schwartz et al. examined the release of drugs from wax matrices into water. They fabricated the tablets by suspending and dissolving the drugs homogenously throughout wax matrices. The group found that drug release data resulted in a straight line when the log of the amount of drug remaining in the matrix was plotted as a function of time (Figure 37) as predicted by first-order release kinetics demonstrated in Equation 6. Interestingly, the rate of release is not significantly altered with different levels of initial drug-loading.[170]

$$\log(W) = \frac{kt}{2.303} + \log(W_0) \qquad \text{[Equation 6]}$$

Where:

W = amount of drug remaining in the tablet

W_0 = initial amount of drug loaded in the tablet

k = first-order rate constant

t = time

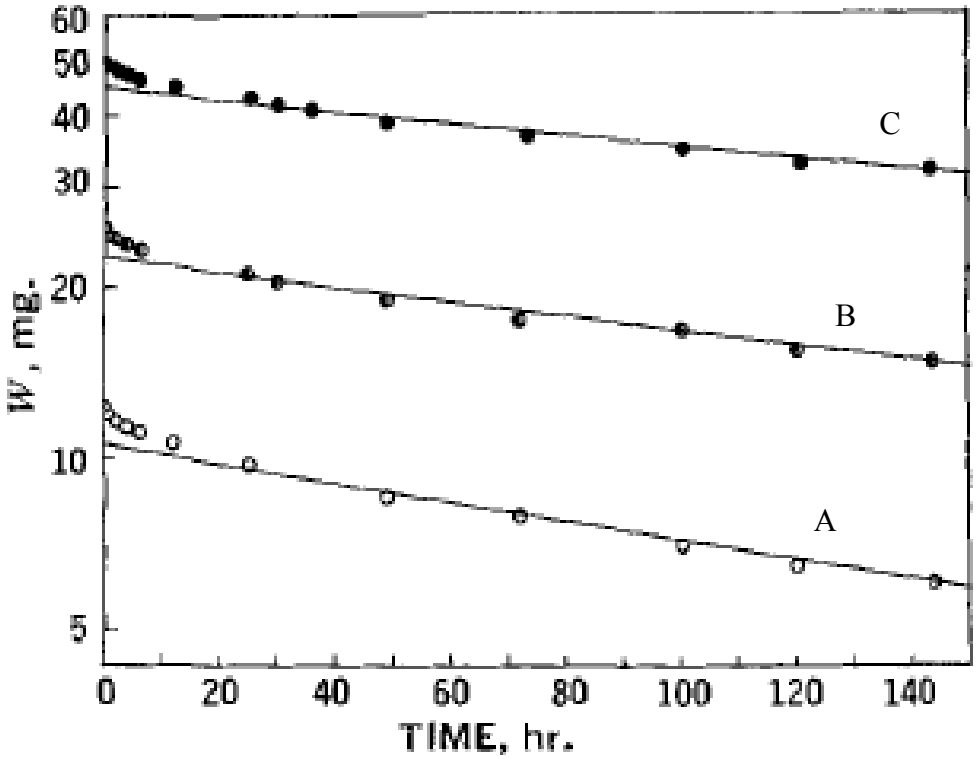

Figure 37: Release of various concentration of the drug from the wax matrix. (A) 5% drug loaded. (B) 10% drug loaded. (C) 20% drug loaded.[170] Reprinted with permission from John Wiley and Sons © 1968.

Goodhart et al. examined the release of water-soluble drugs from a wax matrix timed-release tablet. The group found that phenylpropanolamine hydrochloride initially experienced burst release after which the wax matrix slowly released the drug. After optimizing the fabrication process of the wax matrix tablets, which involved the optimization of the compression force for the tablet, optimal agitation time for the dissolution of drugs in the tablet and the proper size of the tablet, the group tested drug

release from the tablet formulation. Figure 38 depicts the result Goodhart et al. obtained on the release drugs from the wax matrix tablet.

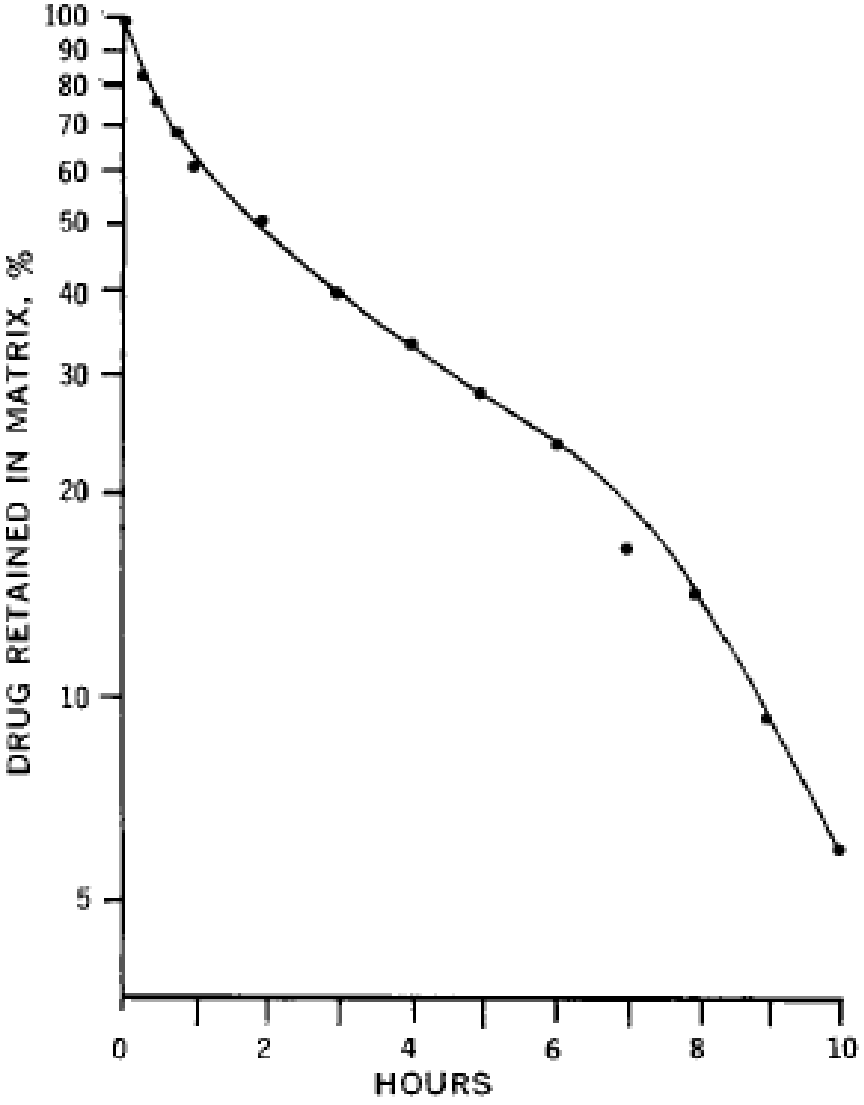

Figure 38: Release of phenylpropanolamine hydrochloride from the wax matrix tablet.[178] Reprinted with permission from John Wiley and Sons © 1974.

Of particular interest, is the interaction between channeling agents and wax. Dakkuri et al. examined the effect of Povidone, also known as polyvinylpyrrolidone (PVP), on the release of tripelennamine hydrochloride from carnauba wax matrices. The group created varying formulations for PVP and wax at concentrations of 0%, 5%, 10%, and 20%. The group found that within the first thirty minutes, drug was released a much quicker rate, in other words, the tablets underwent burst release. They concluded that this was a result of the drugs located on the surface released more rapidly than the drug embedded in the matrix. Then over time, the channeling agent, PVP, allowed for the medium to penetrate the wax matrix and allow for the slow dissolution of drug. Figure 39 depicts the effect of PVP on the release of drugs from the matrix formulations.[171] As

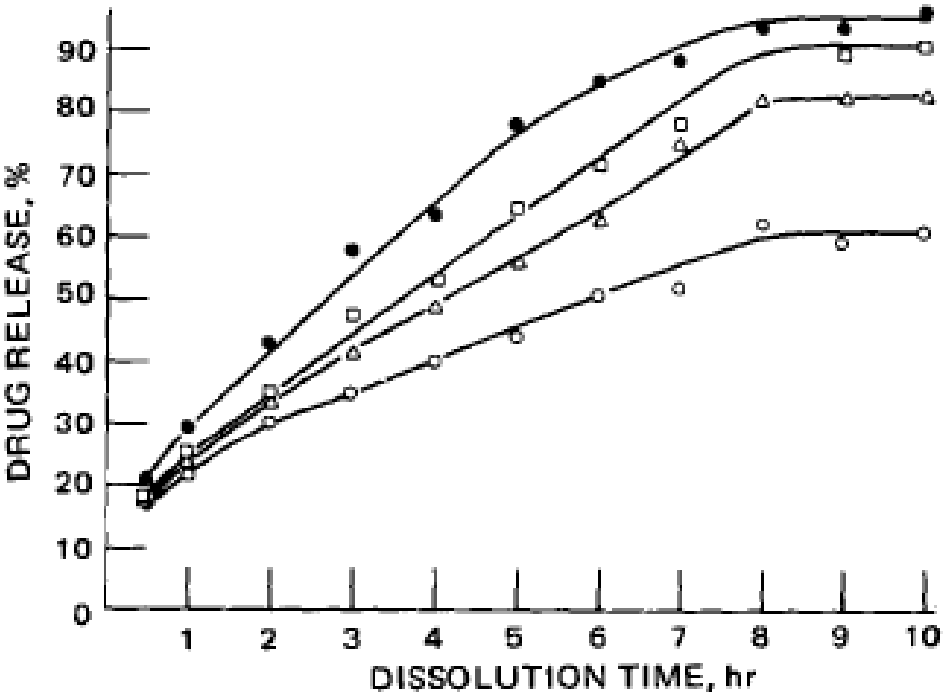

Figure 39: Effect of PVP on the release of drugs from the wax matrix. Key: 0% (open circle). 5% (open triangle). 10% (open square). 20% (closed circle).[171] Reprinted with permission from John Wiley and Sons © 1978.

expected, an increasing concentration of PVP in the wax matrix resulted in an increased

rate of drug release as well as a higher drug release ceiling. This is likely because of the increasing PVP resulting in more water entering the wax matrix to result in the release of drug at a quicker rate. Next, Dakkuri et al. tested the release of drug from the wax-PVP matrix in simulated intestinal fluid and modified intestinal fluid. Figures 40 and 41 depict the results they found after running these experiments.

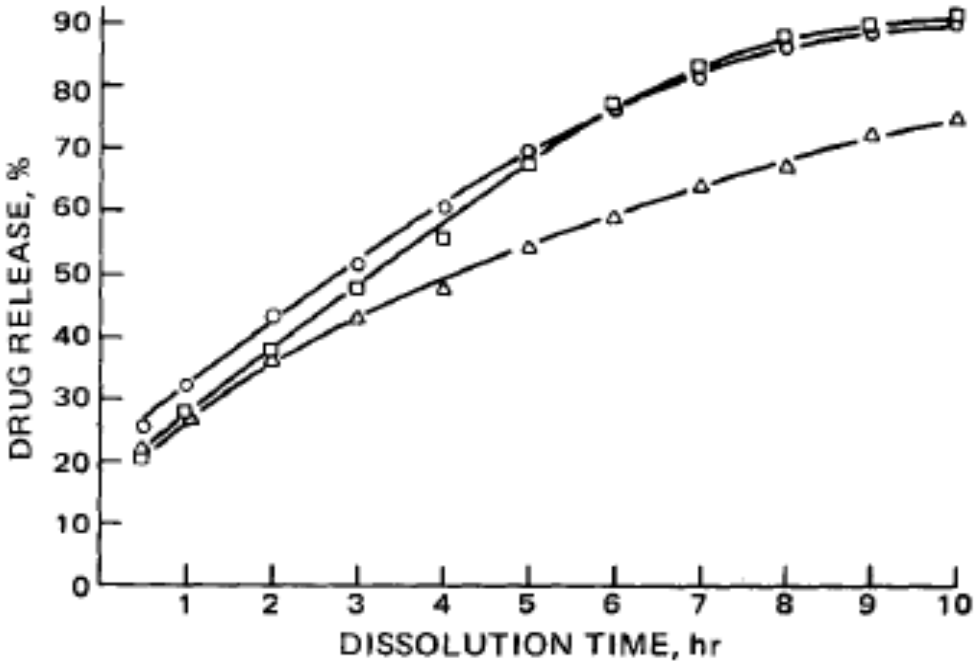

Figure 41: Effect of PVP on the release of drugs from the wax matrix in simulated intestinal fluid. Key: 5% (triangle). 10% (square). 20% (circle).[171] Reprinted with permission from John Wiley and Sons © 1978.

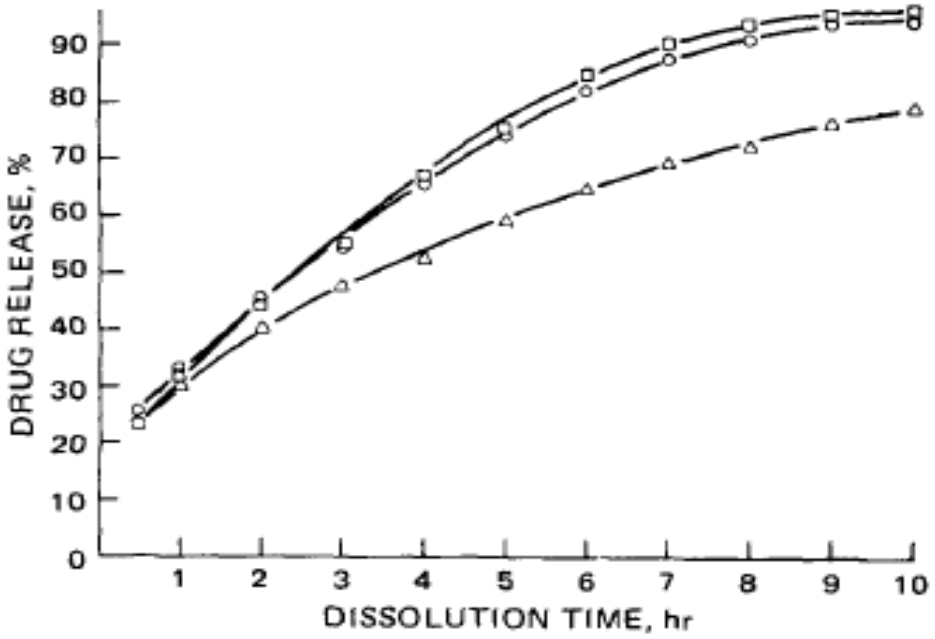

Figure 41: Effect of PVP on the release of drugs from the wax matrix in modified intestinal fluid. Key: 5% (triangle). 10% (square). 20% (circle).[171] Reprinted with permission from John Wiley and Sons © 1978.

The two intestinal fluid experiments resulted in slightly different release rates for the 10% and 20% PVP-wax formulations. The group concluded that 10% was the more effective method for drug release rate in GI fluids.

4.3 Methods

The effect of PVP on the release of drugs from paraffin wax was tested by mixing various concentrations of wax, PVP and model drugs. The two chemical agents that were released from the wax-PVP matrix formulations were fluorescein, a common model drug, and Metformin an antidiabetic.

For the fluorescein experiments, one gram of wax was mixed with six milligrams of fluorescein. Table 1 includes the formulations used in the fluorescein experiments.

Table 1: Recipes for wax-PVP drug release experiments

	Negative Control	Positive Control	5%	10%	15%
Wax	1 gram	1 gram	1 gram	1 gram	1 gram
PVP	0 mg	0 mg	50 mg	100 mg	150 mg
Fluorescein	0 mg	6 mg	6 mg	6 mg	6 mg

After the wax formulation was created in a glass vial, it was mixed overnight at 90ºC and 900RPM. The liquid wax formulation was then cooled at room temperature until solid. Once the formula was solidified, the wax formulation in the glass vial was immersed in 20mL of deionized (DI) water at 37ºC. The glass vials were kept at 37ºC using a hot plate to maintain temperature and a Styrofoam cylinder to insulate the vials so as to keep the entire vial in a 37ºC environment. Measurements were then taken at intermittent time variables by removing 25µL of sample solution, placing it in a 24 well plate and diluting it in 475µL of DI water. The 24 well-plate was then placed in a SpectraMax i3 to

measure the fluorescence at a 475nm excitation wavelength and 510nm emission wavelength. DI water was used as the plate blank. Reference values were also obtained by testing the fluorescence of wax-PVP only samples so as to eliminate any potential interfering spectroscopic data due to PVP. The SpectraMax i3 setting were set to well scan and the software was set to collect 21 data points from each well.

Metformin experiments were formulated in a similar manner as the fluorescein sample, except 200mg of wax was used for each formulation. The absorbance wavelength was set to 250nm. Other SpectraMax i3 settings were kept the same.

Contact angle measurements were obtained by creating wax-PVP formulations, melting them and depositing it on a glass slides. The wax-PVP samples were then spread out evenly over the glass plate using razors. The contact angle was then calculated by collecting images from a goniometer.

4.4 Results and Discussion

Drug release experiments were tested with both fluorescein and metformin. Fluorescein experiments were run three times, while metformin was run twice when it was determined further formulation optimization was required.

4.4.1 Fluorescein Release

Fluorescein was selected a model drug due to its consistent use as a model drug in multiple controlled drug release experiments. Experiment parameters were slightly modeled after theragrippers experiments conducted by Malachowski et al. Total experiments were run for 144 hours. Figure 42 depicts the established standard curve graph and equation.

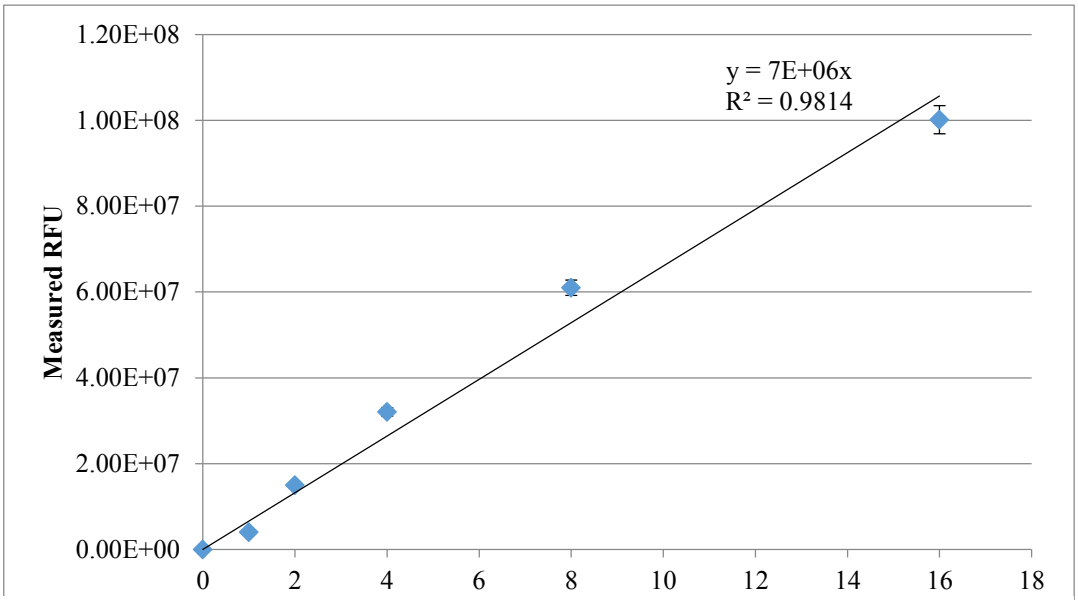

Figure 42: Relative Fluorescence Units (RFU) vs. concentration standard curve. The standard curve results in an the following equation: Concentration = RFU/7E6. The projection line has an R^2 value of .9814 making it a particularly good predictor for all concentrations within and outside of the measured range.

The first six hours of drug release are presented in Figure 43. The data presented is a compilation of the three trials with standard error bars. As presented in Figure 43, 10% wax-PVP results in the least net amount of drug release for the first six hours. All three formulations present burst release, with 10% and 5% PVP formulations bursting release to around 4.5µg/mL while 0% resulted in burst release to around 6µg/mL. By the

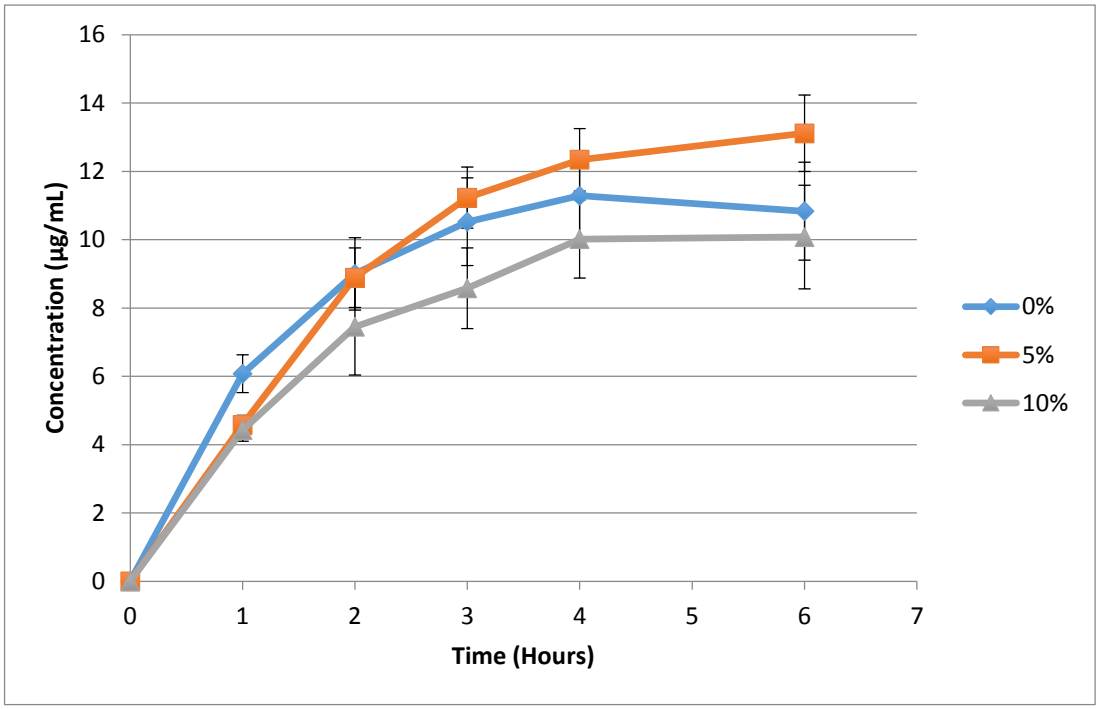

Figure 43: Fluorescein release from wax-PVP over first six hours.

second hour, however, the 5% formulation continues its burst release trajectory to catch up with the control (0%) formulation at around 9µg/mL. From hours two to six, the 5% formulation continues in a upward trajectory, while the control and 10% formulations level off at around four hours, with concentrations of 12µg/mL and 10µg/mL, respectively. The results from the first six hours suggest that the 5% formulation allows for the net most release of fluorescein. It is important to note the standard error bars,

however. As is evident, the standard error bars for each formulation is fairly large at these lower concentrations. Thus, it cannot yet be concluded with certainty that the 5% formulation is indeed the best option for drug release. However, the data from the 6 hour to 144 hour time period in Figure 44 does provide more information on the drug release

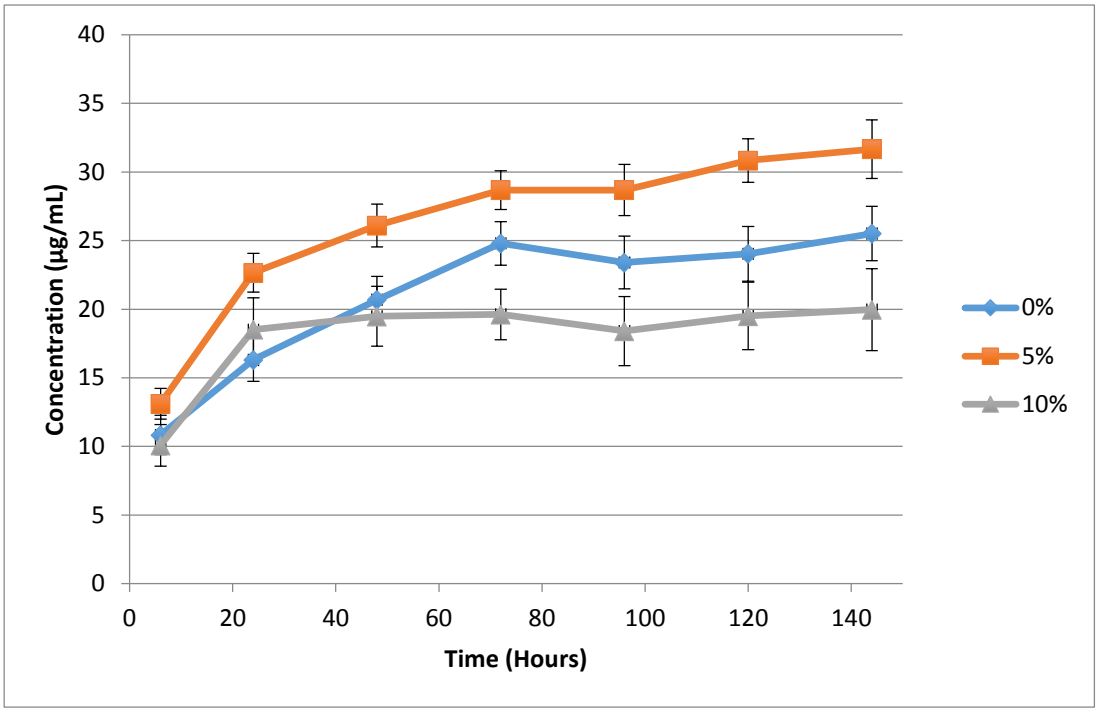

Figure 44: Fluorescein release from 6-144 hours in various wax-PVP formulations.

kinetics for each formulation. For the long-term release of fluorescein, the trend continues for each formulation, with 5% outperforming the other formulations. After 144 hours, the 5% formulation nets a release of 31.66µg/mL in the water solution. With approximately 19.75mL of water remaining in the vial when that sample was collected, that is about 625µg (0.625mg) in the water solution. The initial wax matrix was loaded with 6mg of fluorescein. Thus, the 5% formulation nets a release of approximately 10.42% of the total amount of loaded fluorescein. The control and 10% formulations netted a release of 503.63µg (8.4%) and 389.42µg (6.5%), respectively. The decrease in

release of the model drug in 10% formulations is not what was expected. It is suspected that the extra channeling agent added to much material to the wax matrix and made it more difficult for the fluorescein to exit the matrix or for the surrounding medium, water, to enter the matrix. The underperformance of the 10% formulation compared to the control certainly suggests that the PVP played a large role in hinder fluorescein release rather than an inherent barrier within the wax matrix.

In order to ensure that the fluorescence readings were only indicative of fluorescein release and not PVP release, a reference study was performed. Each formulation was created without adding fluorescein so as to eliminate residual fluorescence as a result of PVP release. The data presented in Figures 43 and 44 is not reduced with the reference values taken into account since the reference values presented very low fluorescence and unstable measurements as exhibited in Figure 45. The Relative Fluorescence Units (RFU) values for the references are significantly lower than the sample RFU values. Furthermore, the inconsistency in the trend data suggests that the RFU values measured are likely due to normal noise measurements rather than PVP.

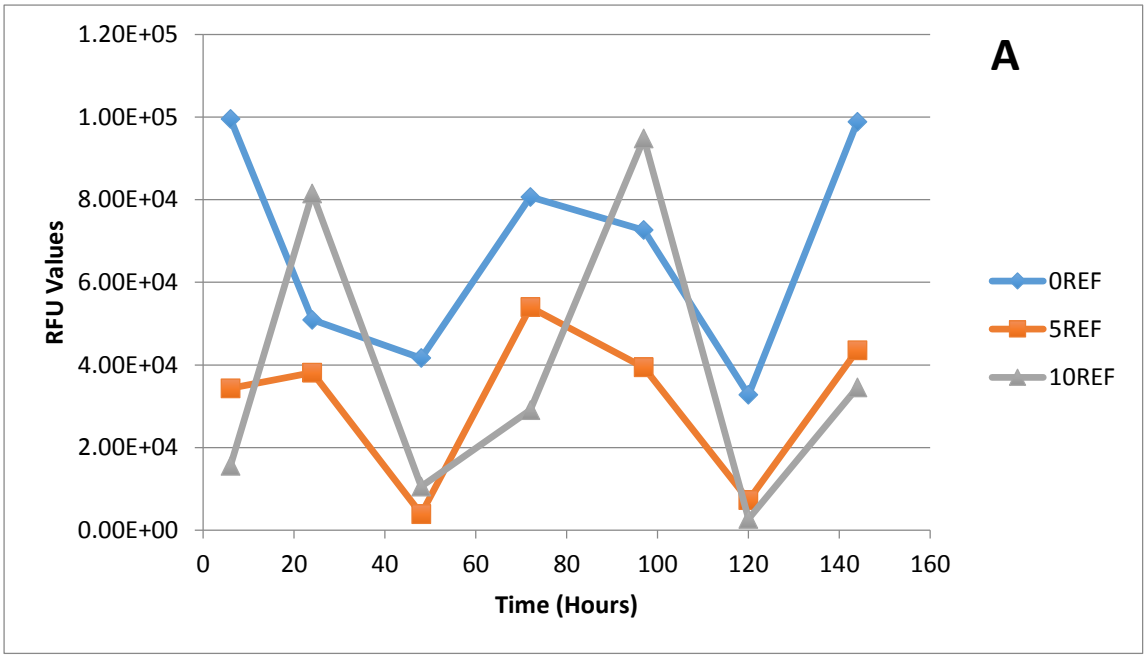

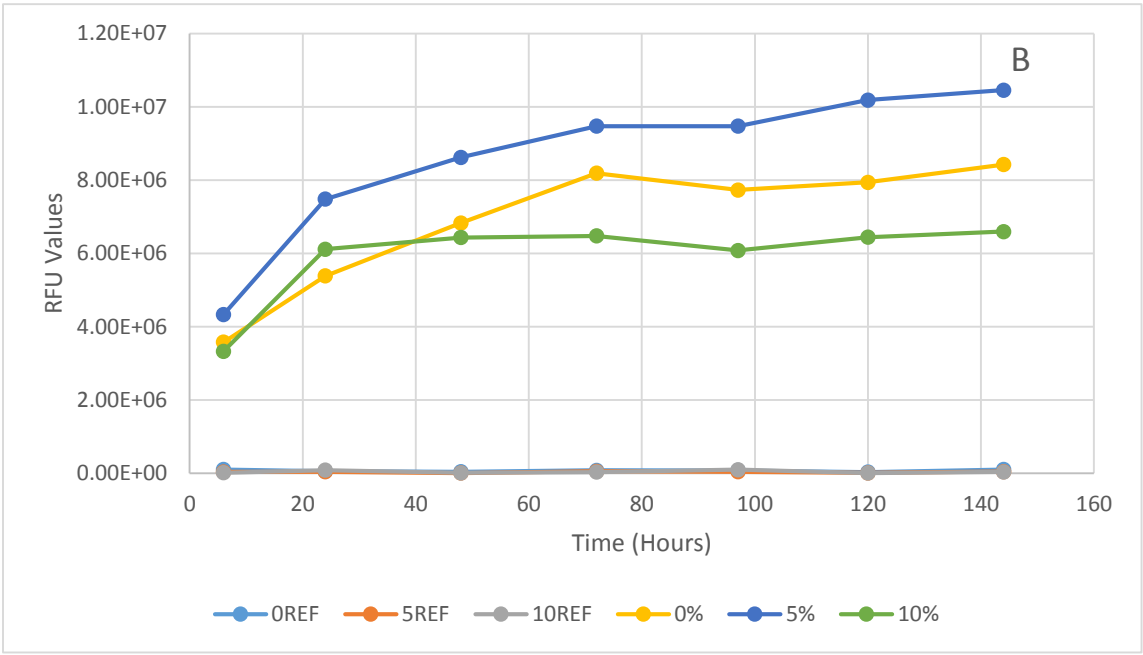

Figure 45: RFU values for wax-PVP only references. (A) RFU values for the references only. As is clearly evident, there is no consistent pattern with the values over the 6-144 hour time period. (B) Comparison of the RFU values for the references compared to the samples. As is evident, the references are significantly smaller than the RFU values due to fluorescein release in the samples.

4.4.2 Metformin Release

Similar to the fluorescein experiments, a metformin standard curve was also established to develop an equation between optical density and concentration as displayed in Figure 46.

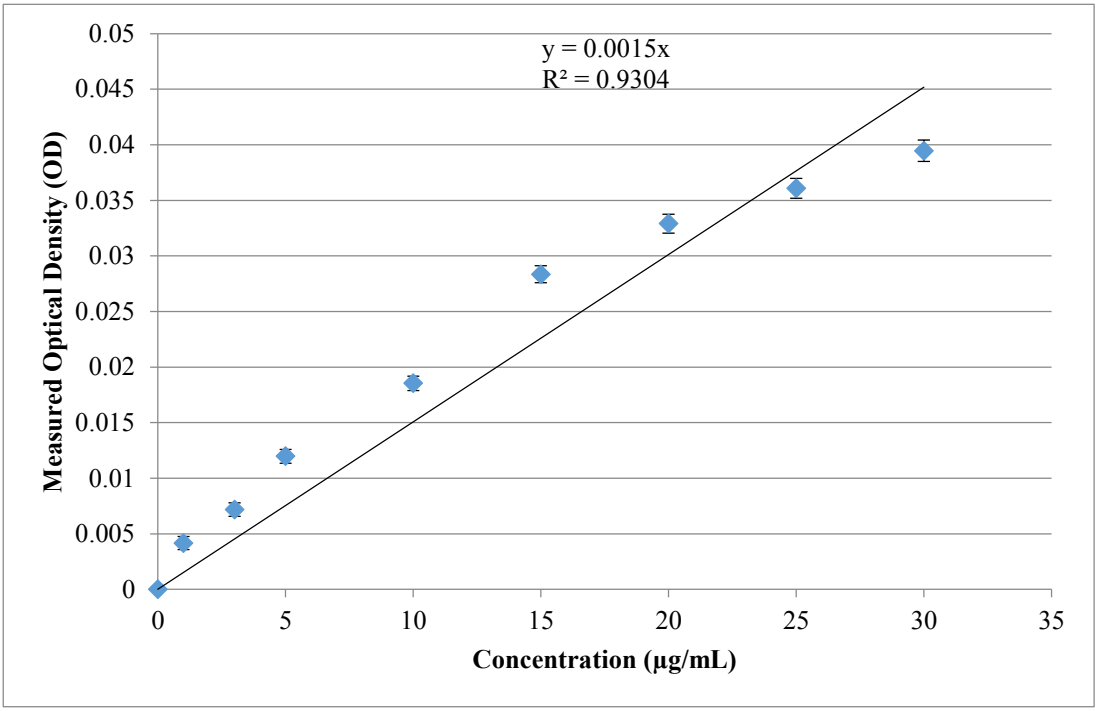

Figure 46: Measured Optical Density (OD) vs. concentration for standard curve equation. Using the data established in the standard curve, the equation relating OD and concentration is as follows: Concentration = OD/.0015. The R^2 value is 0.9304 indicating that the equation is good prediction for measurements within and outside the range.

Figure 47 exhibits one experiment on the release of metformin from the wax-PVP matrices. The data does not indicate any pattern and indicates a significant amount of noise. Furthermore, the optical density measurements reported do not include any reference values to ensure that additional interaction by PVP is accounted for.

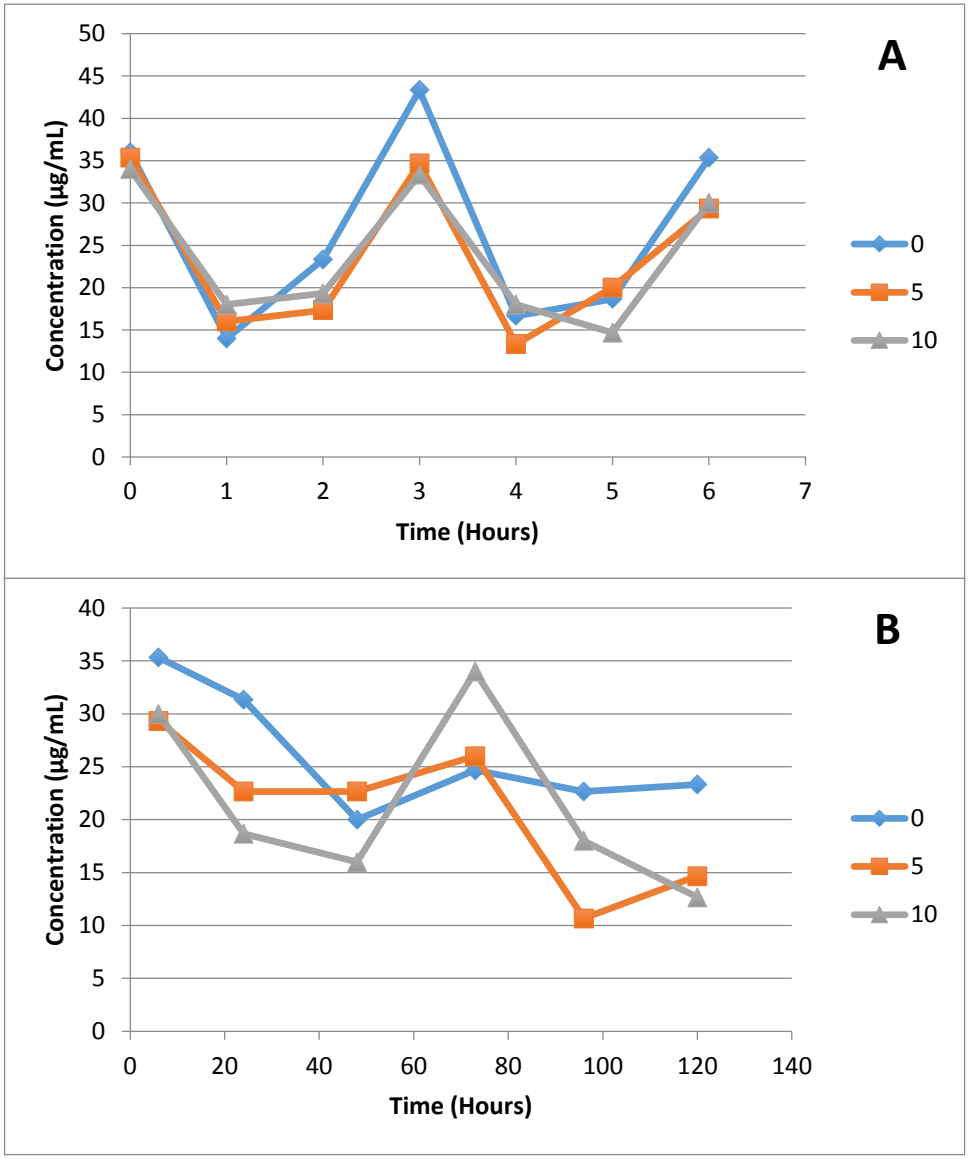

Figure 47: Metformin release from wax-PVP matrix formulations. (A) 6-144 hours does not indicate any clear patterns. Looking at 6-144 hours (B) again does not show any pattern regarding the release of Metformin from the wax-PVP mixture.

An earlier experiment, not included here, indicated some pattern for the metformin release that was consistent with the results from the fluorescein experiments. Again, however, this data was not reduced with reference values taken from wax-PVP matrices to eliminate interaction between absorbance and PVP and does not present any significant conclusive results.

Figure 48 depicts the importance of including a reference value for PVP as the optical density values for the wax-PVP only matrices were high enough to be false negative measurements of PVP.

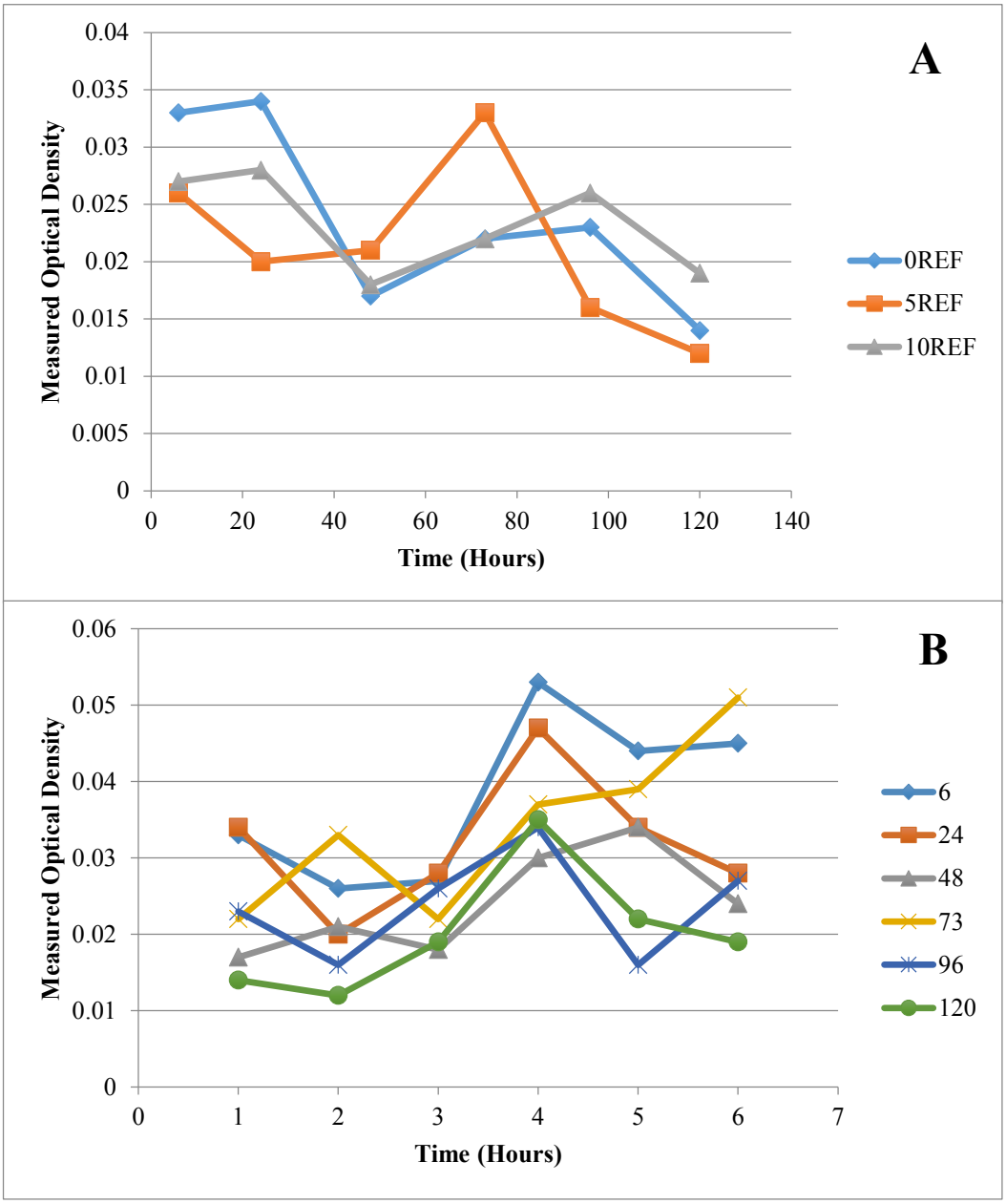

Figure 48: Reference measured optical density values compared to the measured sample values. The measured optical density values for wax-PVP formulations do not apparently exhibit a pattern (A). The measured optical density values for wax-PVP, however, are close to the measured sample values (B).

4.4.3 Contact Angle Measurements

Contact angle measurements were performed using a goniometer. It was suspected that PVP would decrease the hydrophobicity of the wax layer. This is of particular importance for the microgrippers as a less hydrophobic microgripper would have an enhanced ability to attach to the surface of tissue *in vivo.* Figure 49 displays the results from one contact angle measurement experiments. Each data point was measured twenty times resulting in standard error bars.

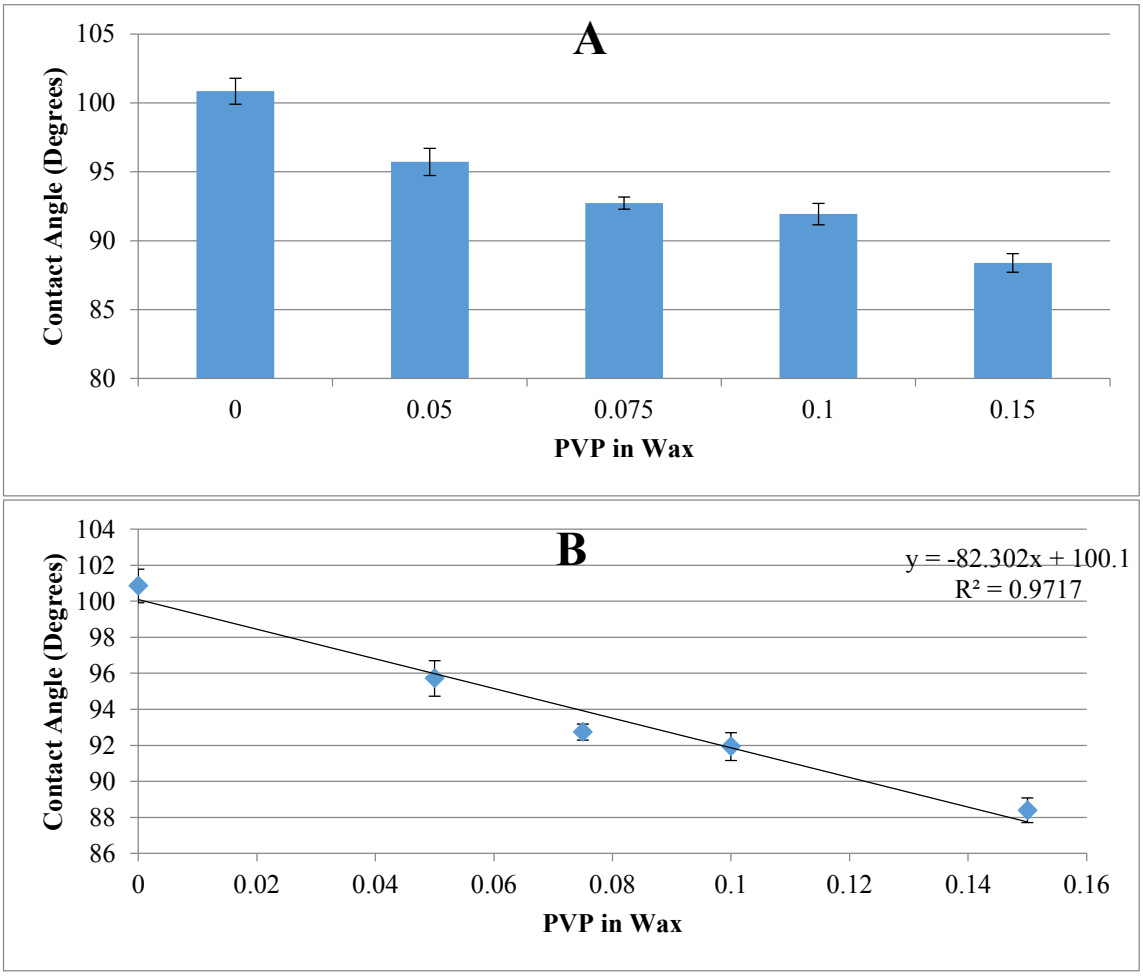

Figure 49: Measured contact angle for each wax-PVP formulation. (A) Bar graph representing the reduction of the contact angle for each wax-PVP formulation. (B) Placed in a linear plot with a linear fit. Key: 0.05 (5%), 0.075 (7.5%), 0.1(10%), and 0.15(15%)

The contact angle measurement does indicate a slight decrease in hydrophobicity for the wax-PVP formulations. In general, however, the decrease in contact angle is not likely significant enough to indicate that this would have a large impact in the forces experienced by microgrippers. Furthermore, the 5% formulation, which is of great interest due to its enhanced fluorescein release characteristics, is not significantly more hydrophilic than the control (0%).

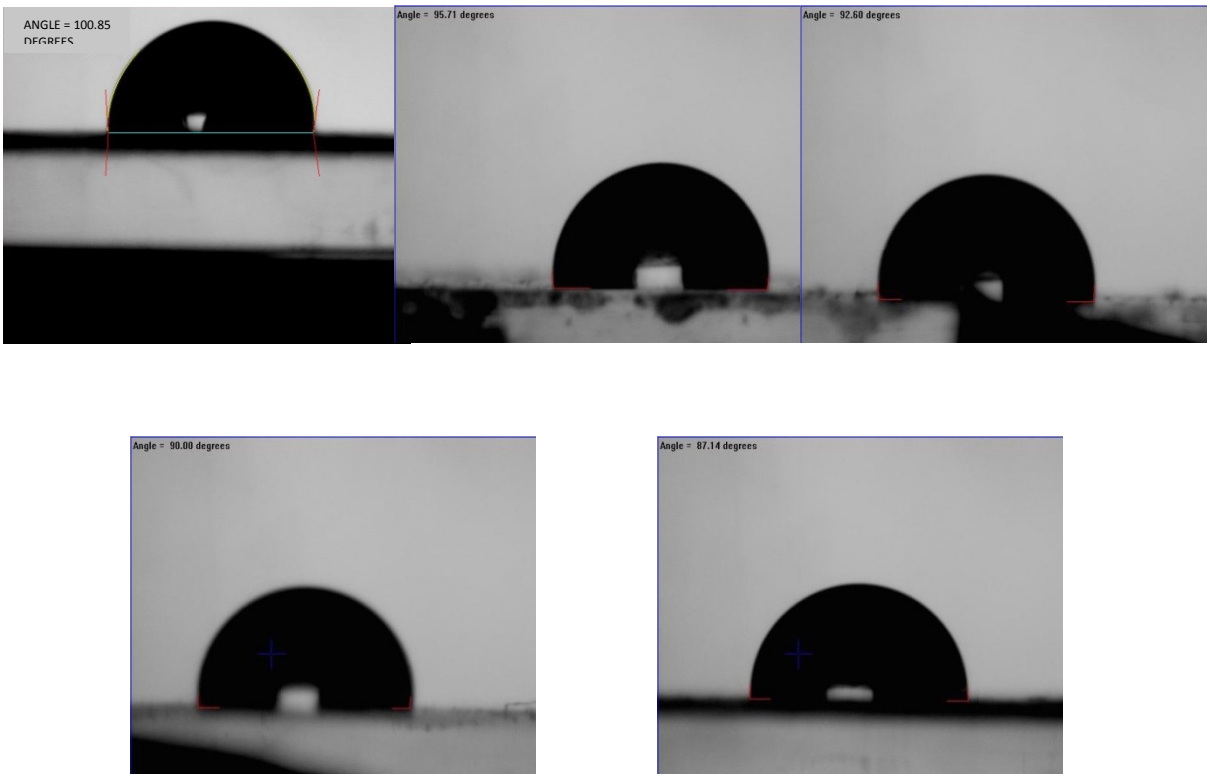

Figure 50: Contact angle images of water on the wax-PVP matrix formulations.

4.5 Conclusion

Paraffin wax has not been extensively studied for the release of drugs. Previous work has extensively studied the release of drugs from natural wax products, namely Carnauba wax. The work from Dakkuri et al. using PVP to utilize channeling agents in order to increase the permeation of the wax matrix, does have some translation to paraffin wax. PVP did indeed increase the release of fluorescein from paraffin. However, Carnauba wax increased the release of drugs with an increasing concentration of PVP, while paraffin wax reached a ceiling at 5%. 10% PVP formulations had the opposite desired effect. Other experiments not reported with even higher concentrations of PVP, 15% and 20% were similar to the drug release profile for 10%. More importantly, future work needs to be done on the release of actual drugs from the wax-PVP formulations. Metformin is a good drug that can be further explored, however, the initial amount of metformin loaded into the matrix needs to be optimized through further experimentation. Furthermore, at the submission of this thesis, the initial fluorescein wax-PVP experiments on microgrippers were being performed. Smaller quantities of wax on microgrippers may very well alter the overall release of drugs from the microgrippers.

Overall, paraffin wax is a good actuation material for microgrippers. Using the work presented in this document can help combine the mechanical actions of paraffin wax, with potential drug or dye release applications for microgrippers. Sustained release should be the first goal for future experiments. Controlled release would be established by optimizing the initial wax and PVP formulations. Additional investigations on the versatility of wax would provide extra information for this purpose.

References

1. Saltzman, M. *Drug Delivery: Engineering Principles for Drug Therapy*. (Oxford University Press, 2001).
2. Kutmalge, M. D., Jadhav, A. N., Ratnaparkhi, M. P. & Chaudhari, S. P. Sustained Release Drug Delivery System. *Pharma Sci. Monit.* **5,** 191–208 (2014).
3. Sicree, B. R., Shaw, J. & Zimmet, P. The Global Burden Diabetes and Impaired Glucose Tolerance. *IDF Diabetes Atlas* 1–105 (2012). doi:10.1097/01.hjr.0000368191.86614.5a
4. Karter, A. J. *et al.* New prescription medication gaps: a comprehensive measure of adherence to new prescriptions. *Health Serv. Res.* **44,** 1640–61 (2009).
5. Guillausseau, P. J. Influence of oral antidiabetic drugs compliance on metabolic control in type 2 diabetes. A survey in general practice. *Diabetes Metab.* **29,** 79–81 (2003).
6. García-Pérez, L.-E., Álvarez, M., Dilla, T., Gil-Guillén, V. & Orozco-Beltrán, D. Adherence to Therapies in Patients with Type 2 Diabetes. *Diabetes Ther.* **4,** 175–194 (2013).
7. Claxton, A. J., Cramer, J. & Pierce, C. A systematic review of the associations between dose regimens and medication compliance. *Clin. Ther.* **23,** 1296–1310 (2001).
8. Shen, S., Jasti, B. & Li, X. in *Standard Handbook of Biomedical Engineering and Design* (2003).
9. Janssen, M., Mihov, G., Welting, T., Thies, J. & Emans, P. Drugs and Polymers for Delivery Systems in OA Joints: Clinical Needs and Opportunities. *Polymers (Basel).* **6,** 799–819 (2014).
10. Zeng, F. *et al.* The impact of value-based benefit design on adherence to diabetes medications: a propensity score-weighted difference in difference evaluation. *Value Health* **13,** 846–52 (2010).
11. Langer, R. New methods of drug delivery. *Science (80-.).* **249,** 1527–1533 (1990).
12. Freiberg, S. & Zhu, X. X. Polymer microspheres for controlled drug release. *Int. J. Pharm.* **282,** 1–18 (2004).
13. Yang, W.-W. & Pierstorff, E. Reservoir-Based Polymer Drug Delivery Systems. *J. Lab. Autom.* **17,** 50–58 (2012).
14. Pinchuk, L. *et al.* Medical applications of poly(styrene-block-isobutylene-block-styrene) ('SIBS'). *Biomaterials* **29,** 448–460 (2008).
15. Patel, H., Panchal, D. R., Patel, U., Brahmbhatt, T. & Suthar, M. Matrix Type Drug Delivery System : A Review. *J. Pharm. Sci. Biosci. Res.* **1,** 143–151 (2011).
16. Nokhodchi, A., Raja, S., Patel, P. & Asare-Addo, K. The role of oral controlled release matrix tablets in drug delivery systems. *Bioimpacts* **2,** 175–87 (2012).
17. Peppas, N. A. & Meadows, D. L. Macromolecular structure and solute diffusion in membranes: An overview of recent theories. *J. Memb. Sci.* **16,** 361–377 (1983).
18. Peppas, N. A. & Reinhart, C. T. SOLUTE DIFFUSION IN SWOLLEN MEMBRANES. Part I. A New Theory. *J. Memb. Sci.* **15,** 275–287 (1983).
19. Bae, K. H., Wang, L.-S. & Kurisawa, M. Injectable biodegradable hydrogels: progress and challenges. *J. Mater. Chem. B* **1,** 5371–5388 (2013).

20. Varma, M. V. S., Kaushal, A. M., Garg, A. & Garg, S. Factors Affecting Mechanism and Kinetics of Drug Release from Matrix-Based Oral Controlled Drug Delivery Systems. *Am. J. Drug Deliv.* **2,** 43–57 (2004).
21. Efentakis, M., Al-Hmoud, H., Buckton, G. & Rajan, Z. The influence of surfactants on drug release from a hydrophobic matrix. *Int. J. Pharm.* **70,** 153–158 (1991).
22. Zuleger, S., Fassihi, R. & Lippold, B. C. Polymer particle erosion controlling drug release. II. Swelling investigations to clarify the release mechanism. *Int. J. Pharm.* **247,** 23–37 (2002).
23. Colombo, P., Bettini, R., Catellani, P. L., Santi, P. & Peppas, N. a. Drug volume fraction profile in the gel phase and drug release kinetics in hydroxypropylmethyl cellulose matrices containing a soluble drug. *Eur. J. Pharm. Sci.* **9,** 33–40 (1999).
24. Tahara, K., Yamamoto, K. & Nishihata, T. Overall mechanism behind matrix sustained release (SR) tablets prepared with hydroxypropyl methylcellulose 2910. *J. Control. Release* **35,** 59–66 (1995).
25. Flynn, G. L., Yalkowsky, S. H. & Roseman, T. J. Mass transport phenomena and models. Theoretical concepts. *J. Pharm. Sci.* **63,** 479–510 (1974).
26. Rafiee-Tehrani, M. & Sadegh-Shobeiri, N. Effect of Various Polymers on Formulation of Controlled Release (CR) Ibuprofen Tablets by Fluid Bed Technique. *Drug Dev. Ind. Pharm.* **21,** 1193–1202 (1995).
27. French, D., Hagland, B. & Himmelstein, K. Measurement of Drug Concentration Profiles in Carbopol Matrices and Correlation to Drug Release Kinetics. *Pharm. Res.* **11,** S287 (1995).
28. Kristmundsdottir, T., Ingvarsdottir, K. & Saemundsdottir, G. Chitosan matrix tablets: The influence of excipients on drug release. *Drug Dev. Ind. Pharm.* **21,** 1591–1598 (1995).
29. Siepmann, J., Podual, K., Sriwongjanya, M., Peppas, N. A. & Bodmeier, R. A new model describing the swelling and drug release kinetics from hydroxypropyl methylcellulose tablets. *J. Pharm. Sci.* **88,** 65–72 (1999).
30. Duddu, S. P., Vakilynejad, M., Jamali, F. & Grant, D. J. W. Stereoselective Dissolution of Propranolol Hydrochloride from Hydroxypropyl Methylcellulose Matrices. *Pharm. Res.* **10,** 1648–1653 (1993).
31. Chebli, C. & Cartilier, L. Release and Swelling Kinetics of Substituted Amylose Matrices. *J. Pharm. Sci.* **54,** 51–54 (1999).
32. Bettini, R. *et al.* Translocation of drug particles in HPMC matrix gel layer : effect of drug solubility and influence on release rate. *J. Control. Release* **70,** 383–391 (2001).
33. Skoug, J. W., Mikelsons, M. V., Vigneron, C. N. & Stemm, N. . Qualitative evaluation of the mechanism of release of matrix sustained release dosage forms by measurement of polymer release. *J. Control. Release* **27,** 227–245 (1993).
34. Chebli, C., Cartilier, L. & Hartman, N. G. Substituted amylose as a matrix for sustained-drug release: a biodegradation study. *International journal of pharmaceutics* **222,** 183–9 (2001).
35. Peppas, N. A. & Sahlin, J. J. A simple equation for the description of solute release. III. Coupling of diffusion and relaxation. *Int. J. Pharm.* **57,** 169–172

(1989).
36. Delargy, A., Timmins, P. & Mnchom, C. Evaluation of the release mechanism of a pH-independen matrix for controlled release. *Control. Release Bioactivated Mater.* **17,** (1990).
37. Hino, T. & Ford, J. L. Effect of nicotinamide on the properties of aqueous HPMC solutions. *Int. J. Pharm.* **226,** 53–60 (2001).
38. Nellore, R. V, Rekhi, G. S., Hussain, a S., Tillman, L. G. & Augsburger, L. L. Development of metoprolol tartrate extended-release matrix tablet formulations for regulatory policy consideration. *J. Control. Release* **50,** 247–256 (1998).
39. Mulye, N. & Turco, S. An examination of assumptions underlying the first-order kinetic model for release of water soluble drugs from dicalcium phosphate dihydrate matrices. *Drug Dev. Ind. Pharm.* **22,** 673–679 (1996).
40. Heng, P. W. S., Chan, L. W., Easterbrook, M. G. & Li, X. Investigation of the influence of mean HPMC particle size and number of polymer particles on the release of aspirin from swellable hydrophilic matrix tablets. *J. Control. Release* **76,** 39–49 (2001).
41. Feely, L. C. & Davis, S. S. Influence of surfactants on drug release from hydroxypropylmethylcellulose matrices. *Int. J. Pharm.* **41,** 83–90 (1988).
42. Hussain, A., Johnson, R. & Shivanand, P. Effects of blending a non-ionic and an anionic cellulose ether polymer on drug release from hydrophilic matrix capsule. *Drug Dev. Ind. Pharm.* **20,** 2645–2657 (1994).
43. Rao, K., Devi, K. & Buri, P. Cellulose matrices for zero-order release of soluble drugs. *Drug Dev. Ind. Pharm.* **14,** 2299–2320 (1988).
44. Siepmann, J., Streubel, A. & Peppas, N. a. Understanding and predicting drug delivery from hydrophilic matrix tablets using the 'sequential layer' model. *Pharm. Res.* **19,** 306–314 (2002).
45. Grayson, A. C. R. *et al.* A BioMEMS review: MEMS technology for physiologically integrated devices. *Proc. IEEE* **92,** 6–21 (2004).
46. Nuxoll, E. BioMEMS in drug delivery. *Adv. Drug Deliv. Rev.* **65,** 1611–1625 (2013).
47. Nir, Y., Paz, A., Sabo, E. & Potasman, I. Fear of injections in young adults: Prevalence and associations. *Am. J. Trop. Med. Hyg.* **68,** 341–344 (2003).
48. Hamilton, J. G. Needle phobia: a neglected diagnosis. *J. Fam. Pract.* **41,** 169–75 (1995).
49. Champion, R. H., Burton, J. L. & Ebling, F. J. G. *Textbook of Dermatology*. (Blackwell Scientific, 1991).
50. Babiuk, S., Baca-Estrada, M., Babiuk, L. a., Ewen, C. & Foldvari, M. Cutaneous vaccination: The skin as an immunologically active tissue and the challenge of antigen delivery. *J. Control. Release* **66,** 199–214 (2000).
51. Prausnitz, M. R., Mikszta, J. A., Cormier, M. & Andrianov, A. K. Microneedle-based vaccines. *Curr. Top. Microbiol. Immunol.* **333,** 369–93 (2009).
52. Kim, Y. C., Park, J. H. & Prausnitz, M. R. Microneedles for drug and vaccine delivery. *Adv. Drug Deliv. Rev.* **64,** 1547–1568 (2012).
53. Van Der Maaden, K., Jiskoot, W. & Bouwstra, J. Microneedle technologies for (trans)dermal drug and vaccine delivery. *J. Control. Release* **161,** 645–655 (2012).

54. Donnelly, R. F., Raj Singh, T. R. & Woolfson, a D. Microneedle-based drug delivery systems: microfabrication, drug delivery, and safety. *Drug Deliv.* **17,** 187–207 (2010).
55. Sachdeva, V. & Banga, A. K. Microneedles and their applications. *Recent Pat. Drug Deliv. Formul.* **5,** 95–132 (2011).
56. Banga, A. K. Microporation applications for enhancing drug delivery. *Expert Opin. Drug Deliv.* **6,** 343–354 (2009).
57. Sivamani, R. K., Liepmann, D. & Maibach, H. I. Microneedles and transdermal applications. *Expert Opin. Drug Deliv.* **4,** 19–25 (2007).
58. Henry, S., McAllister, D. V., Allen, M. G. & Prausnitz, M. R. Microfabricated microneedles: A novel approach to transdermal drug delivery. *J. Pharm. Sci.* **87,** 922–925 (1998).
59. Roxhed, N., Gasser, T. C., Griss, P., Holzapfel, G. a. & Stemme, G. Penetration-enhanced ultrasharp microneedles and prediction on skin interaction for efficient transdermal drug delivery. *J. Microelectromechanical Syst.* **16,** 1429–1440 (2007).
60. Wilke, N., Mulcahy, a., Ye, S. R. & Morrissey, a. Process optimization and characterization of silicon microneedles fabricated by wet etch technology. *Microelectronics J.* **36,** 650–656 (2005).
61. Coulman, S. A. *et al.* Microneedle mediated delivery of nanoparticles into human skin. *Int. J. Pharm.* **366,** 190–200 (2009).
62. Martanto, W. *et al.* Transdermal delivery of insulin using microneedles in vivo. *Pharm. Res.* **21,** 947–952 (2004).
63. Mikszta, J. a *et al.* Improved genetic immunization via micromechanical disruption of skin-barrier function and targeted epidermal delivery. *Nat. Med.* **8,** 415–419 (2002).
64. Wermeling, D. P. *et al.* Microneedles permit transdermal delivery of a skin-impermeant medication to humans. *Proc. Natl. Acad. Sci. U. S. A.* **105,** 2058–2063 (2008).
65. Qiu, Y., Gao, Y., Hu, K. & Li, F. Enhancement of skin permeation of docetaxel: a novel approach combining microneedle and elastic liposomes. *J. Control. Release* **129,** 144–150 (2008).
66. Yerramreddy, T. R., Milewski, M., Penthala, N. R., Stinchcomb, A. L. & Crooks, P. a. Novel 3-O-pegylated carboxylate and 3-O-pegylated carbamate prodrugs of naltrexone for microneedle-enhanced transdermal delivery. *Bioorganic Med. Chem. Lett.* **20,** 3280–3283 (2010).
67. Milewski, M., Pinninti, R. R. & Stinchcomb, A. L. Naltrexone salt selection for enhanced transdermal permeation through microneedle-treated skin. *J. Pharm. Sci.* **101,** 2777–2786 (2012).
68. Gupta, J., Gill, H. S., Andrews, S. N. & Prausnitz, M. R. Kinetics of skin resealing after insertion of microneedles in human subjects. *J. Control. Release* **154,** 148–155 (2011).
69. Kalluri, H. & Banga, A. K. Formation and closure of microchannels in skin following microporation. *Pharm. Res.* **28,** 82–94 (2011).
70. Banks, S. L., Paudel, K. S., Brogden, N. K., Loftin, C. D. & Stinchcomb, A. L. Diclofenac enables prolonged delivery of naltrexone through microneedle-treated

skin. *Pharm. Res.* **28,** 1211–1219 (2011).
71. Aust, M. C. *et al.* Percutaneous collagen induction: minimally invasive skin rejuvenation without risk of hyperpigmentation-fact or fiction? *Plast. Reconstr. Surg.* **122,** 1553–1563 (2008).
72. www.dermaroller.com. at <www.dermaroller.com>
73. Gill, H. S. & Prausnitz, M. R. Coating formulations for microneedles. *Pharm. Res.* **24,** 1369–1380 (2007).
74. Gill, H. S. & Prausnitz, M. R. Coated microneedles for transdermal delivery. *J. Control. Release* **117,** 227–237 (2007).
75. Kim, Y. C. *et al.* Enhanced memory responses to seasonal H1N1 influenza vaccination of the skin with the use of vaccine-coated microneedles. *J Infect Dis* **201,** 190–198 (2010).
76. Kim, Y.-C., Quan, F.-S., Compans, R. W., Kang, S.-M. & Prausnitz, M. R. Formulation of microneedles coated with influenza virus-like particle vaccine. *AAPS PharmSciTech* **11,** 1193–1201 (2010).
77. Gill, H. S. & Prausnitz, M. R. Pocketed microneedles for drug delivery to the skin. *J. Phys. Chem. Solids* **69,** 1537–1541 (2008).
78. Han, M. *et al.* Improvement in antigen-delivery using fabrication of a grooves-embedded microneedle array. *Sensors Actuators B Chem.* **137,** 274–280 (2009).
79. Saurer, E. M., Flessner, R. M., Sullivan, S. P., Prausnitz, M. R. & Lynn, D. M. Layer-by-layer assembly of DNA- and protein-containing films on microneedles for drug delivery to the skin. *Biomacromolecules* **11,** 3136–3143 (2010).
80. DeMuth, P. C., Su, X., Samuel, R. E., Hammond, P. T. & Irvine, D. J. Nano-layered microneedles for transcutaneous delivery of polymer nanoparticles and plasmid DNA. *Adv. Mater.* **22,** 4851–6 (2010).
81. Cormier, M. *et al.* Transdermal delivery of desmopressin using a coated microneedle array patch system. *J. Control. Release* **97,** 503–511 (2004).
82. Vrdoljak, A. *et al.* Coated microneedle arrays for transcutaneous delivery of live virus vaccines. *J. Control. Release* **159,** 34–42 (2012).
83. Peters, E. E., Ameri, M., Wang, X., Maa, Y.-F. & Daddona, P. E. Erythropoietin-coated ZP-microneedle transdermal system: preclinical formulation, stability, and delivery. *Pharm. Res.* **29,** 1618–26 (2012).
84. Zhu, Q. *et al.* Immunization by vaccine-coated microneedle arrays protects against lethal influenza virus challenge. *Proc. Natl. Acad. Sci. U. S. A.* **106,** 7968–73 (2009).
85. Quan, F.-S., Kim, Y.-C., Compans, R. W., Prausnitz, M. R. & Kang, S.-M. Dose sparing enabled by skin immunization with influenza virus-like particle vaccine using microneedles. *J. Control. Release* **147,** 326–32 (2010).
86. Koutsonanos, D. G. *et al.* Delivery of subunit influenza vaccine to skin with microneedles improves immunogenicity and long-lived protection. *Sci. Rep.* **2,** 1–10 (2012).
87. Kim, Y.-C. *et al.* Increased immunogenicity of avian influenza DNA vaccine delivered to the skin using a microneedle patch. *Eur. J. Pharm. Biopharm.* **81,** 239–47 (2012).
88. Chen, X. *et al.* Site-Selectively Coated, Densely-Packed Microprojection Array

Patches for Targeted Delivery of Vaccines to Skin. *Adv. Funct. Mater.* **21,** 464–473 (2011).
89. Weldon, W. C. *et al.* Effect of adjuvants on responses to skin immunization by microneedles coated with influenza subunit vaccine. *PLoS One* **7,** e41501 (2012).
90. Andrianov, A. K. *et al.* Poly[di(carboxylatophenoxy)phosphazene] is a potent adjuvant for intradermal immunization. *Proc. Natl. Acad. Sci. U. S. A.* **106,** 18936–41 (2009).
91. Gill, H. S., Söderholm, J., Prausnitz, M. R. & Sällberg, M. Cutaneous vaccination using microneedles coated with hepatitis C DNA vaccine. *Gene Ther.* **17,** 811–4 (2010).
92. Pearton, M. *et al.* Microneedle delivery of plasmid DNA to living human skin: Formulation coating, skin insertion and gene expression. *J. Control. Release* **160,** 561–9 (2012).
93. Choi, H. J. *et al.* Stability of influenza vaccine coated onto microneedles. *Biomaterials* **33,** 3756–3769 (2012).
94. Martanto, W., Moore, J. S., Couse, T. & Prausnitz, M. R. Mechanism of fluid infusion during microneedle insertion and retraction. *J. Control. Release* **112,** 357–361 (2006).
95. Wang, P. M., Cornwell, M., Hill, J. & Prausnitz, M. R. Precise microinjection into skin using hollow microneedles. *J. Invest. Dermatol.* **126,** 1080–1087 (2006).
96. Gupta, J., Park, S. S., Bondy, B., Felner, E. I. & Prausnitz, M. R. Infusion pressure and pain during microneedle injection into skin of human subjects. *Biomaterials* **32,** 6823–6831 (2011).
97. Verbaan, F. J. *et al.* Improved piercing of microneedle arrays in dermatomed human skin by an impact insertion method. *J. Control. Release* **128,** 80–88 (2008).
98. Yang, M. & Zahn, J. D. Microneedle insertion force reduction using vibratory actuation. *Biomedical microdevices* **6,** 177–82 (2004).
99. Brazzle, J., Papautsky, I. & Frazier, A. B. Micromachined needle arrays for drug delivery or fluid extraction. *IEEE Eng. Med. Biol. Mag.* **18,** 53–58 (1999).
100. Chandrasekaran, S., Brazzle, J. D. & Frazier, A. B. Surface Micromachined Metallic Microneedles. *J. Microelectromechanical Syst.* **12,** 281–288 (2003).
101. Zahn, J. D., Trebotich, D. & Liepmann, D. Microdialysis microneedles for continuous medical monitoring. *Biomed. Microdevices* **7,** 59–69 (2005).
102. Zahn, J., Talbot, N., Liepmann, D. & Pisano, A. Microfabricated polysilicon microneedles for minimally invasive biomedical devices. *Biomed. Microdevices* 295–303 (2000). doi:10.1023/A:1009907306184
103. Lin, L. W. & Pisano, A. P. Silicon-processed microneedles. *J. Microelectromechanical Syst.* **8,** 78–84 (1999).
104. Zahn, J. D., Deshmukh, A., Pisano, A. P. & Liepmann, D. Continuous on-chip micropumping for microneedle enhanced drug delivery. *Biomed. Microdevices* **6,** 183–190 (2004).
105. Ling Teo, M. A., Shearwood, C., Ng, K. C., Lu, J. & Moochhala, S. In vitro and in vivo characterization of MEMS microneedles. *Biomed. Microdevices* **7,** 47–52 (2005).
106. Baron, N., Passave, J., Guichardaz, B. & Cabodevila, G. Investigations of

development process of high hollow beveled microneedles using a combination of ICP RIE and dicing saw. *Microsyst. Technol.* **14,** 1475–1480 (2008).
107. Stoeber, B. & Liepmann, D. Arrays of hollow out-of-plane microneedles for drug delivery. *J. Microelectromechanical Syst.* **14,** 472–479 (2005).
108. Gardeniers, H. J. G. E. *et al.* Silicon micromachined hollow microneedles for transdermal liquid transport. *J. Microelectromechanical Syst.* **12,** 855–862 (2003).
109. Davis, S. P., Martanto, W., Allen, M. G. & Prausnitz, M. R. Hollow metal microneedles for insulin delivery to diabetic rats. *IEEE Trans. Biomed. Eng.* **52,** 909–915 (2005).
110. Roxhed, N., Griss, P. & Stemme, G. Membrane-sealed hollow microneedles and related administration schemes for transdermal drug delivery. *Biomed. Microdevices* **10,** 271–9 (2008).
111. Nordquist, L., Roxhed, N., Griss, P. & Stemme, G. Novel microneedle patches for active insulin delivery are efficient in maintaining glycaemic control: An initial comparison with subcutaneous administration. *Pharm. Res.* **24,** 1381–1388 (2007).
112. Cachemaille, A. & Piveteau, L. D. Simple and reliable intra-dermal injections. *ONdrugDelivery* 18–21 (2012). at <http://www.scopus.com/inward/record.url?eid=2-s2.0-84864449823&partnerID=tZOtx3y1>
113. Debiotech. at <http://www.debiotech.com/newsite/page/index.php?page=home>
114. NanoPass Technologies Ltd. at <http://www.nanopass.com/>
115. U.S. Food & Drug Administration 510(k) Summary. at <http://www.accessdata.fda.gov/cdrh_docs/pdf9/k092746.pdf>
116. Intradermal Versus Intramuscular Polio Vaccine Booster in HIV-Infected Subjects - Full Text View - ClinicalTrials.gov. at <https://www.clinicaltrials.gov/ct2/show/NCT01686503>
117. Pharmacokinetic Comparison of Intradermal Versus Sub-cutaneous Insulin and Glucagon Delivery in Type 1 Diabetes - Full Text View - ClinicalTrials.gov. at <https://www.clinicaltrials.gov/ct2/show/NCT01684956>
118. Matthaei, M. *et al.* Systematic assessment of microneedle injection into the mouse cornea. *Eur. J. Med. Res.* **17,** 19 (2012).
119. Patel, S. R. *et al.* Targeted administration into the suprachoroidal space using a microneedle for drug delivery to the posterior segment of the eye. *Invest. Ophthalmol. Vis. Sci.* **53,** 4433–41 (2012).
120. Reed, M. L. *et al.* Micromechanical devices for intravascular drug delivery. *J. Pharm. Sci.* **87,** 1387–94 (1998).
121. Choi, C. K., Kim, J. B., Jang, E. H., Youn, Y.-N. & Ryu, W. H. Curved biodegradable microneedles for vascular drug delivery. *Small* **8,** 2483–8 (2012).
122. Kumar, V. & Banga, A. K. Modulated iontophoretic delivery of small and large molecules through microchannels. *Int. J. Pharm.* **434,** 106–14 (2012).
123. Vemulapalli, V. *et al.* In vivo iontophoretic delivery of salmon calcitonin across microporated skin. *J. Pharm. Sci.* **101,** 2861–9 (2012).
124. Chen, H. *et al.* Iontophoresis-driven penetration of nanovesicles through microneedle-induced skin microchannels for enhancing transdermal delivery of insulin. *J. Control. Release* **139,** 63–72 (2009).

125. Choi, S.-O. *et al.* Intracellular protein delivery and gene transfection by electroporation using a microneedle electrode array. *Small* **8,** 1081–91 (2012).
126. Lee, K., Kim, J. D., Lee, C. Y., Her, S. & Jung, H. A high-capacity, hybrid electro-microneedle for in-situ cutaneous gene transfer. *Biomaterials* **32,** 7705–10 (2011).
127. Tao, S. L. & Desai, T. a. Gastrointestinal patch systems for oral drug delivery. *Drug Discov. Today* **10,** 909–915 (2005).
128. Lavelle, E. C. Targeted delivery of drugs to the gastrointestinal tract. *Critical reviews in therapeutic drug carrier systems* **18,** 341–86 (2001).
129. Ponchel, G. & Irache, J. M. Specific and non-specific bioadhesive particulate systems for oral delivery to the gastrointestinal tract. *Adv. Drug Deliv. Rev.* **34,** 191–219 (1998).
130. Eaimtrakarn, S. *et al.* Retention and transit of intestinal mucoadhesive films in rat small intestine. *Int. J. Pharm.* **224,** 61–67 (2001).
131. Saffran, M. *et al.* Biodegradable azopolymer coating for oral delivery of peptide drugs. *Biochem. Soc. Trans.* **18,** 752–4 (1990).
132. Iwanaga, K. *et al.* Application of surface-coated liposomes for oral delivery of peptide: Effects of coating the liposome's surface on the GI transit of insulin. *J. Pharm. Sci.* **88,** 248–252 (1999).
133. Jerry, N., Anitha, Y., Sharma, C. P. & Sony, P. In vivo absorption studies of insulin from an oral delivery system. *Drug Deliv.* **8,** 19–23 (2001).
134. Florence, A. T. & Hussain, N. Transcytosis of nanoparticle and dendrimer delivery systems: evolving vistas. *Adv. Drug Deliv. Rev.* **50,** S69–S89 (2001).
135. McClean, S. *et al.* Binding and uptake of biodegradable poly-DL-lactide micro- and nanoparticles in intestinal epithelia. *Eur. J. Pharm. Sci.* **6,** 153–63 (1998).
136. GRÖNING, R., WERNER, M., BERNTGEN, M. & GEORGARAKIS, M. Peroral controlled release dosage forms with internal magnets and extracorporal magnetic guidance : investigations into the renal elimination of riboflavin. *Eur. J. Pharm. Biopharm.* **42,** 25–28
137. Häfeli, U. O. Magnetically modulated therapeutic systems. *Int. J. Pharm.* **277,** 19–24 (2004).
138. Dorkoosh, F. A. *et al.* Feasibility study on the retention of superporous hydrogel composite polymer in the intestinal tract of man using scintigraphy. *J. Control. Release* **99,** 199–206 (2004).
139. Timmermans, J. & Moës, A. J. Factors controlling the buoyancy and gastric retention capabilities of floating matrix capsules: new data for reconsidering the controversy. *J. Pharm. Sci.* **83,** 18–24 (1994).
140. Säkkinen, M. *et al.* Gamma scintigraphic evaluation of the fate of microcrystalline chitosan granules in human stomach. *Eur. J. Pharm. Biopharm.* **57,** 133–143 (2004).
141. Peppas, N. a. & Huang, Y. Nanoscale technology of mucoadhesive interactions. *Adv. Drug Deliv. Rev.* **56,** 1675–1687 (2004).
142. Roldo, M., Hornof, M., Caliceti, P. & Bernkop-Schnürch, A. Mucoadhesive thiolated chitosans as platforms for oral controlled drug delivery: Synthesis and in vitro evaluation. *Eur. J. Pharm. Biopharm.* **57,** 115–121 (2004).
143. Krauland, A. H., Guggi, D. & Bernkop-Schnürch, A. Oral insulin delivery: The

potential of thiolated chitosan-insulin tablets on non-diabetic rats. *J. Contr. Rel.* **95,** 547–555 (2004).
144. Arangoa, M. *et al.* Bioadhesive potential of gliadin nanoparticulate systems. *Eur. J. Pharm. Sci.* **11,** 333–341 (2000).
145. Lehr, C. M. Lectin-mediated drug delivery: The second generation of bioadhesives. *J. Control. Release* **65,** 19–29 (2000).
146. Naisbett, B. & Woodley, J. The potential use of tomato lectin for oral drug delivery: 4. Immunological consequences. *Int. J. Pharm.* **120,** 247–254 (1995).
147. Davaran, S., Rashidi, M. R., Khandaghi, R. & Hashemi, M. Development of a novel prolonged-release nicotine transdermal patch. *Pharmacol. Res.* **51,** 233–237 (2005).
148. Burkman, R. T. The transdermal contraceptive system. *Am. J. Obstet. Gynecol.* **190,** S49–53 (2004).
149. Thomas, B. J. & Finnin, B. C. The transdermal revolution. *Drug Discov. Today* **9,** 697–703 (2004).
150. Nagai, T. & Machida, Y. Buccal delivery systems using hydrogels. *Adv. Drug Deliv. Rev.* **11,** 179–191 (1993).
151. Anders, R. & Merkle, H. P. Evaluation of laminated muco-adhesive patches for buccal drug delivery. *Int. J. Pharm.* **49,** 231–240 (1989).
152. Merkle, H. . & Wolany, G. J. . Mucoadhesive patches for buccal peptide administration. *Buccal Nasal Adm. as an Altern. to Parenter. Adm.* 110–124 (1996).
153. Remuñán-López, C., Portero, A., Vila-Jato, J. L. & Alonso, M. J. Design and evaluation of chitosan/ethylcellulose mucoadhesive bilayered devices for buccal drug delivery. *J. Control. Release* **55,** 143–52 (1998).
154. Eaimtrakarn, S. *et al.* Gastrointestinal mucoadhesive patch system (GI-MAPS) for oral administration of G-CSF, a model protein. *Biomaterials* **23,** 145–152 (2002).
155. Takada, K. *et al.* Pharmacological activity of tablets containing recombinant human granulocyte colony-stimulating factor (rhG-CSF) in rats. *Int. J. Pharm.* **101,** 89–96 (1994).
156. TAKAYA, T., IKEDA, C., IMAGAWA, N., NIWA, K. & TAKADA, K. Development of a Colon Delivery Capsule and the Pharmacological Activity of Recombinant Human Granulocyte Colony-stimulating Factor (rhG-CSF) in Beagle Dogs. *J. Pharm. Pharmacol.* **47,** 474–478 (1995).
157. Eaimtrakarn, S. *et al.* Possibility of a patch system as a new oral delivery system. *Int. J. Pharm.* **250,** 111–117 (2003).
158. Eaimtrakarn, S. *et al.* Evaluation of gastrointestinal transit characteristics of oral patch preparation using caffeine as a model drug in human volunteers. *Drug Metab. Pharmacokinet.* **17,** 284–91 (2002).
159. Shen, Z. & Mitragotri, S. Intestinal patches for oral drug delivery. *Pharm. Res.* **19,** 391–395 (2002).
160. Fernandes, R. & Gracias, D. H. Self-folding polymeric containers for encapsulation and delivery of drugs. *Adv. Drug Deliv. Rev.* **64,** 1579–1589 (2012).
161. Randall, C. L., Leong, T. G., Bassik, N. & Gracias, D. H. 3D lithographically fabricated nanoliter containers for drug delivery. *Adv. Drug Deliv. Rev.* **59,** 1547–

1561 (2007).
162. Boncheva, M. *et al.* Magnetic self-assembly of three-dimensional surfaces from planar sheets. *Proc. Natl. Acad. Sci. U. S. A.* **102,** 3924–3929 (2005).
163. Bassik, N. *et al.* Enzymatically triggered actuation of miniaturized tools. *J. Am. Chem. Soc.* **132,** 16314–7 (2010).
164. Leong, T. G. *et al.* Tetherless thermobiochemically actuated microgrippers. *Proc. Natl. Acad. Sci. U. S. A.* **106,** 703–708 (2009).
165. He, H., Guan, J. & Lee, J. L. An oral delivery device based on self-folding hydrogels. *J. Control. Release* **110,** 339–46 (2006).
166. Kalinin, Y. V., Randhawa, J. S. & Gracias, D. H. Three-dimensional chemical patterns for cellular self-organization. *Angew. Chemie - Int. Ed.* **50,** 2549–2553 (2011).
167. Malachowski, K. *et al.* Stimuli-Responsive Theragrippers for Chemomechanical Controlled Release. *Angew. Chem. Int. Ed. Engl.* **53,** 1–6 (2014).
168. Freund, M., Csikós, R., Keszthelyi, S. & Mózes, G. *Paraffin products - properties, technologies, applications*. *New York* (1982). doi:10.1016/S0376-7361(08)70148-1
169. Huang, H. P., Mehta, S. C., Radebaugh, G. W. & Fawzi, M. B. Mechanism of Drug-Release from an Acrylic Polymer-Wax Matrix Tablet. *J Pharm Sci* **83,** 795–797 (1994).
170. Schwartz, B. J. B., Simonelli, A. P. & Higuchi, W. I. Drug Release from Wax Matrices. **274,** 274–277 (1964).
171. Dakkuri, A., Butler, D. & DeLuca, P. Sustained Release from Inert Wax Matrixes III: Effect of Povidone on Tripelennamine Hydrochloride Release. *J. Pharm. Sci.* **67,** 357–360 (1978).
172. Roiter, Y. & Minko, S. AFM single molecule experiments at the solid-liquid interface: In situ conformation of adsorbed flexible polyelectrolyte chains. *J. Am. Chem. Soc.* **127,** 15688–15689 (2005).
173. Suh, H., Shin, J. & Kim, Y.-C. Microneedle patches for vaccine delivery. *Clin. Exp. Vaccine Res.* **3,** 42–9 (2014).
174. DeMuth, P. C. *et al.* Polymer multilayer tattooing for enhanced DNA vaccination. *Nat. Mater.* **12,** 367–76 (2013).
175. Gittard, S. D. *et al.* Multiphoton microscopy of transdermal quantum dot delivery using two photon polymerization-fabricated polymer microneedles. *Faraday Discuss.* **149,** 171–85; discussion 227–45 (2011).
176. Wokovich, A. M., Prodduturi, S., Doub, W. H., Hussain, A. S. & Buhse, L. F. Transdermal drug delivery system (TDDS) adhesion as a critical safety, efficacy and quality attribute. *Eur. J. Pharm. Biopharm.* **64,** 1–8 (2006).
177. Googana & Emad. Paraffin Wax. (201AD). at <http://www.googana.com/paraffin-wax/>
178. Goodhart, F. W., McCoy, R. H. & Ninger, F. C. Release of a water-soluble drug from a wax matrix timed-release tablet. *J. Pharm. Sci.* **63,** 1748–1751 (1974).

Parth U. Patel

Phone: 913-901-7623
E-Mail: ppatel35@jhu.edu

Education

Johns Hopkins University (Baltimore, MD) **December 2014-December 2015**
Degree: M.S.E in Chemical and Biomolecular Engineering

Johns Hopkins University (Baltimore, MD) **August 2011-December 2014**

Degree: B.S in Chemical and Biomolecular Engineering
- Concentration in Molecular and Cellular Bioengineering

Blue Valley High School (Stilwell, KS) **August 2007-May 2011**
Degree: Diploma

Research/Design Experience

Easy Suds Venture **February 2014-Present**

- Worked in a team to design and build the Easy Suds device
- Received $1000 at the Entrepreneurship Week Business Plan competition hosted by BME EDGE and Innovation Factory (Awarded to 1 out of 20 teams)
- Received $5000 grant from Venturewell Stage 1 E-Team Grant

Masters Research – Gracias Lab **September 2014 – Present**

- Worked on micro structured/fabricated drug delivery device
- Extensive work with hydrogels and various biodegradable polymers

Undergraduate Research – Gerecht Lab **October 2011-September 2014**

- Worked extensively with stem cells and performed research in vascular regeneration and endothelial differentiation
- Received the Chemical and Biomolecular Engineering Undergraduate Research Award in May 2013 for my involvement in research in the Institute for NanoBioTechnology specifically in Gerecht Lab
- Received $2500 through the Provost Undergraduate Research Award (PURA) to expand on my own research project titled: Hypoxia Induced Differentiation of Human Induced Pluripotent Stem Cells.
- Publication: Co-author on "Low oxygen tension enhances endothelial fate of human pluripotent stem cells" in the *Atherosclerosis, Thrombosis and Vascular Biology Journal*

Research at University of Kansas – Farassati Lab **June-September 2010**

- Worked primarily with pancreatic cancer cells
- Observed various protein expressions of cancer cells using a western blot analysis and genetic analysis

Laboratory Equipment and Techniques: Live cell culture (including stem cell culture), immunofluorescent staining, fluorescent microscopy, RT-PCR, Western Blot, Magnetic Activated Cell Sorting, Hypoxia induced cell culture, and live-cell imaging